GENERAL ELECTRIC PETTRACE CYCLOTRON AS A NEUTRON SOURCE FOR BORON NEUTRON CAPTURE THERAPY

A Dissertation

by

ANDREY BOSKO

Submitted to the Office of Graduate Studies of
Texas A&M University
in partial fulfillment of the requirements for the degree of

DOCTOR OF PHILOSOPHY

August 2005

Major Subject: Nuclear Engineering

GENERAL ELECTRIC PETTRACE CYCLOTRON AS A NEUTRON SOURCE FOR BORON NEUTRON CAPTURE THERAPY

A Dissertation

by

ANDREY BOSKO

Submitted to the Office of Graduate Studies of
Texas A&M University
in partial fulfillment of the requirements for the degree of

DOCTOR OF PHILOSOPHY

Approved by:

Chair of Committee,	W. Daniel Reece
Committee Members,	Michael D. Devous
	Leslie A. Braby
	John R. Ford
	Michael A. Walker
Head of Department,	William E. Burchill

August 2005

Major Subject: Nuclear Engineering

ABSTRACT

General Electric PETtrace Cyclotron as a Neutron Source

for Boron Neutron Capture Therapy. (August 2005)

Andrey Bosko, B.S., Moscow Engineering-Physics Institute;

M.S., Moscow Engineering-Physics Institute

Chair of Advisory Committee: Dr. W. Daniel Reece

This research investigates the use of a PETtrace cyclotron produced by General Electric (GE) as a neutron source for boron neutron capture therapy (BNCT). The GE PETtrace was chosen for this investigation because this type of cyclotron is popular among nuclear pharmacies and clinics in many countries; it is compact and reliable; it produces protons with energies high enough to produce neutrons with appropriate energy and fluence rate for BNCT and it does not require significant changes in design to provide neutrons. In particular, the standard PETtrace ^{18}O target is considered. The cyclotron efficiency may be significantly increased if unused neutrons produced during radioisotopes production could be utilized for other medical modalities such as BNCT at the same time.

The resulting dose from the radiation emitted from the target is evaluated using the Monte Carlo radiation transport code MCNP at several depths in a brain phantom for different scattering geometries. Four different moderating materials of various thicknesses were considered: light water, carbon, heavy water, and Fluental^{TM}. The fluence rate tally was used to calculate photon and neutron dose, by applying fluence

rate-to-dose conversion factors.

Fifteen different geometries were considered and a 30-cm thick heavy water moderator was chosen as the most suitable for BNCT with the GE PETtrace cyclotron. According to the Brookhaven Medical Research Reactor (BMRR) protocol, the maximum dose to the normal brain is set to 12.5 RBEGy, which for the conditions of using a heavy water moderator, assuming a 60 μA beam current, would be reached with a treatment time of 258 min. Results showed that using a PETtrace cyclotron in this configuration provides a therapeutic ratio of about 2.4 for depths up to 4 cm inside a brain phantom. Further increase of beam current proposed by GE should significantly improve the beam quality or the treatment time and allow treating tumors at greater depths.

ACKNOWLEDGMENTS

I would like to acknowledge the support of many people who helped me complete this effort. Special thanks go to my committee chairman, Dr. W. Daniel Reece, for his helpful overseeing of this project and continued technical advice. I could not accomplish my degree without his help and support as a Director of the Nuclear Science Center. I must also mention the assistance that my committee members, Dr. Michael D. Devous and Dr. Michael A. Walker, have given in their careful review of this document. I would also like to thank Drs. Leslie A. Braby and John R. Ford for their reviews, discussions and comments on this dissertation. My special thanks to Dr. John W. Poston for his invaluable help in the preparation of this manuscript.

I would also like to extend my thanks to my parents, without whose encouragement it would not have been possible for me to reach this level of academic achievement. Finally, I wish to thank my wife, Alina, for all of the love, understanding and support that she gave me through the last three years.

TABLE OF CONTENTS

CHAPTER Page

LIST OF FIGURES

FIGURE Page

LIST OF TABLES

TABLE Page

CHAPTER I

INTRODUCTION

Neutron capture therapy (NCT) is a radiation therapy that uses nuclides that have a high capture cross-section for thermal neutrons. This capture reaction, followed by disintegration, can result in high energy deposition in the vicinity of reaction site. If such nuclides are introduced selectively into tumor cells, it is possible to destroy the tumor and largely spare the surrounding normal tissue. The principles of this method were described in the middle of 1930's. Shortly after the discovery of the neutron by J. Chadwick in 1932 and the description of the $^{10}B(n,\alpha)^{7}Li$-reaction by Taylor and Goldhaber in 1935, the basic idea to use neutron capture reactions in cancer treatment was published by Locher, an biophysicist with the Franklin Institute in 1936. "In particular, there exist the possibilities of introducing small quantities of strong neutron absorbers into the regions where it is desired to liberate ionization energy (a simple illustration would be the injection of a soluble, non-toxic compound of boron, lithium, gadolinium, or gold into a superficial cancer, followed by bombardment with slow neutrons)."

A number of nuclides exists that have a large absorption cross-section for thermal neutrons and some of these are listed in Table I-1. Most of these nuclides interact with thermal neutrons by the (n,γ) reaction.

This dissertation follows the style of *Physics in Medicine and Biology*.

This type of reaction results in gamma-ray emission and the resulting gammas can penetrate tissue easily, depositing their energy not only in the tumor but in healthy tissue. Thus, these nuclides are not suitable for NCT. But some nuclides may be of interest for NCT, such as ^{6}Li and ^{235}U. One of the limitations in using these nuclides is their toxicity.

Table I-1. Nuclide properties.

Nuclides	Interaction	Cross-section σ_{th} (barns)
^{3}He	(n,p)	5333
^{6}Li	(n,α)	941
^{10}B	(n,α)	3840
^{113}Cd	(n,γ)	20600
^{151}Eu	(n,γ)	9200
^{155}Gd	(n,γ)	61000
^{157}Gd	(n,γ)	255000
^{174}Hf	(n,γ)	530
^{199}Hg	(n,γ)	2200
^{235}U	(n,f)	585
^{241}Pu	(n,f)	1010
^{242}Am	(n,f)	7000

Most experimental work and clinical approaches in NCT have been based on ^{10}B. The first experiments using ^{10}B-NCT were performed in 1940 by Kruger and included in-vitro tumor treatment with boric acid and irradiation. Other researchers investigated the efficiency of NCT in-vivo after injection of boric acid or boron in an oily suspension into a mouse sarcoma. Several years later the treatment of brain tumors was proposed

based on selective uptake of a boron compound by the tumor. Data suggested that the tumor does not have a blood-brain barrier while healthy tissue does. This absence of a blood-brain barrier can lead to higher boron concentrations in brain tumors compared to that in healthy brain tissues.

The first clinical trials in the USA, conducted from 1951 to 1961 using ^{10}B, failed. Later, it became clear that the major reason for this failure was low ^{10}B concentration in the tumor.

Elastic scattering of neutrons and the $^{14}N(n,p)^{14}C$ and $^{1}H(n,\gamma)^{2}H$, nuclear reactions produce recoil nuclei and γ-rays during exposure to neutrons. Although the neutron capture cross-sections for hydrogen and nitrogen are much lower than that for ^{10}B, hydrogen and nitrogen are present in such high concentrations that their neutron capture background contribute significantly to the total absorbed dose. This background and low specificity lead to a low therapeutic ratio.

Despite these early failures, Dr. Hatanaka, a Japanese neurosurgeon who received training with Dr. Sweet at Massachusetts General Hospital at Harvard University, returned to Japan in 1968 and continued to develop the technique. He used a new boron drug BSH ($Na_2{}^{10}B_{12}H_{11}SH$, sodium borocaptate), that concentrated selectively in tumors. Using this drug he performed open-skull irradiation of brain tumors using thermal neutron beams (energy < 0.025 eV) to reach the target without losing significant amounts of the thermal beam. Several groups worked at different reactors using this technique and treated over 200 patients with some encouraging results. At the same time, great progress was achieved in synthesis of boron-containing

compounds enriched in the ^{10}B isotope. These compounds, introduced into a patient's blood, produce in tumor cells a ^{10}B isotope concentration up to 40 mg/g, more than three times larger than that in normal tissue cells. This enables selective destruction of malignant tumors. The Japanese experience and recent advances in the evaluation of tumor-affinitive boron-containing drugs have spurred renewed interest in NCT and now, boron neutron capture therapy (BNCT) is under active investigation all over the world.

This type of therapy is the most promising for curing certain malignant tumors, especially therapy for glioblastoma multiforme and melanoma. Forty to fifty percent of primary central nervous system tumors are gliomas. Approximately 50% of these are glioblastoma multiforme and 7% are astrocytomas. Glioblastoma multiforme refers to a malignant neoplasm with abundant glial pleomorphism, numerous mitotic figures and giant cells, vascular hyperplasia, and focal areas of necrosis. Occurring most commonly in the fifth through seventh decades, glioblastoma multiforme usually develops in the cerebral hemispheres (more often in the frontal lobes than the temporal lobes or basal ganglia) but almost never in the cerebellum. It grows as an irregular mass in the white matter and infiltrates the surrounding parenchyma by coursing along white matter tracts, frequently involving the corpus callosum and crossing the midline to produce the characteristic "butterfly" appearance, see Figure I-1. About one out of 20,000 people every year is afflicted by glioblastoma multiforme. The disease is always fatal and is hard to treat; death usually comes within six months of onset. Surgery and conventional radiation therapies may prolong life for as much as a year but do not stop the spread of tumors throughout the brain.

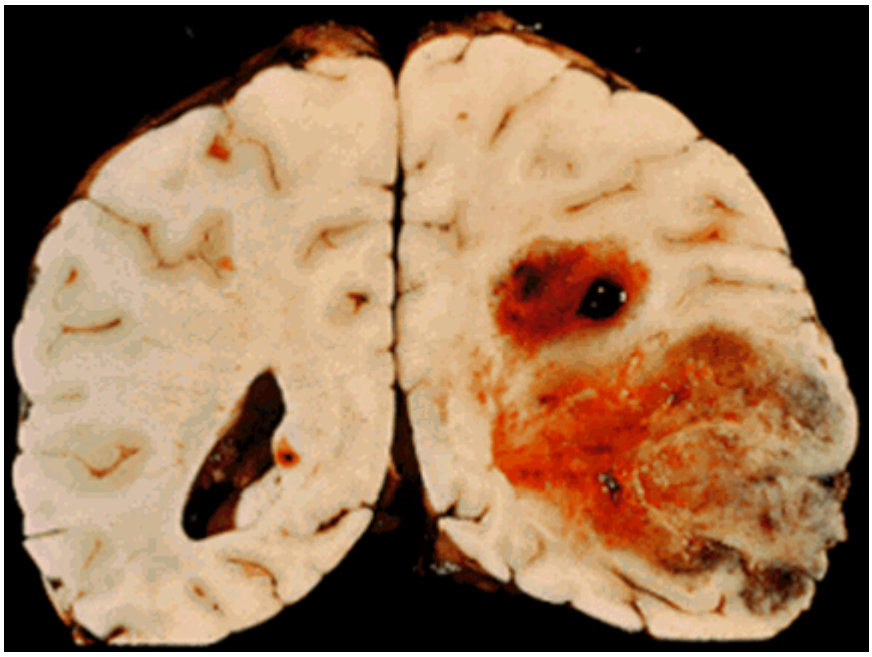

Figure I-1. Glioblastoma multiforme.

For these tumor types BNCT is perhaps the only option. B-10, when in or near tumor cells, disintegrates after capturing a neutron from an epithermal neutron beam. During disintegration high energy particles are produced and these particles deposit a large amount of energy in relatively short distances, effectively destroying the molecular bonds along their paths (see Figure I-2). If any of the paths leads through a cell nucleus, the resulting damage to DNA will likely prevent further cell proliferation. As the ranges of the α-particle and the ^{7}Li nucleus in tissue are comparable to the size of a typical tumor cell, the damage is limited to those cells that accumulate boron. This means that BNCT will make it possible to selectively destroy tumor cells if they will have higher ^{10}B concentration than healthy ones.

Historically, the best source of neutrons at the energy and fluence rate levels

required for BNCT was a nuclear reactor. BNCT research has used the Brookhaven Medical Research Reactor (BMRR), the Massachusetts Institute of Technology Reactor (MITR), reactors at the National Engineer Laboratory in Idaho, and other facilities. The advantage of a reactor is that the neutrons from reactors are relatively cheap discounting capital costs. The disadvantages of reactor are that the capital costs are very high and reactors are too complicated for an ordinary clinic to operate, so these clinics cannot afford to build and maintain a small nuclear reactor to use as a neutron source.

Another approach to this problem is to use particle accelerators. These machines can accelerate protons to the required energies for the reaction and the bombarded target emits neutrons at rates and energy levels appropriate for BNCT. These accelerators are cheaper, easier to operate, and pose less overall risk than nuclear reactors. Accelerator neutron sources are well understood and implemented in a number of research facilities.

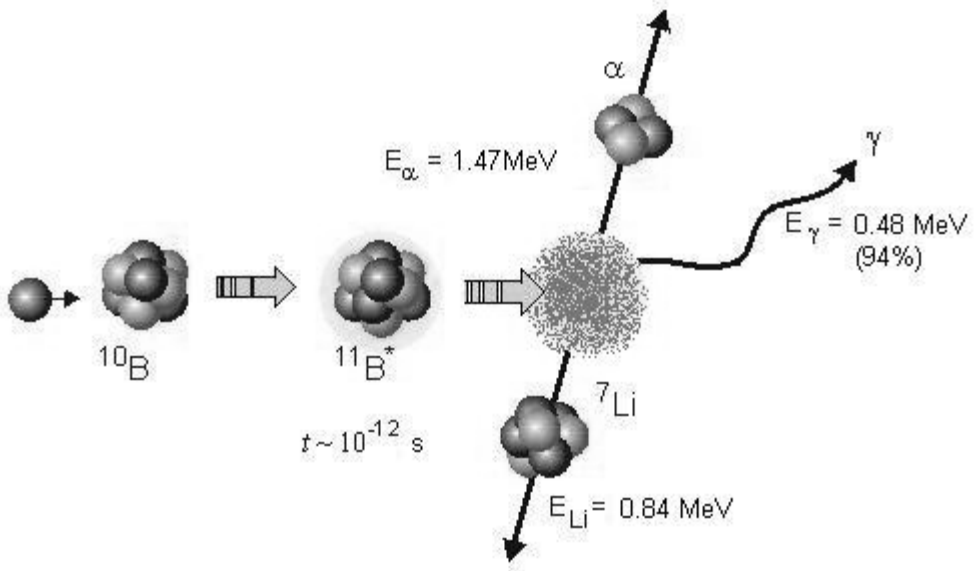

Figure I-2. $^{10}B(n,\alpha)^7Li$ reaction.

CHAPTER II

THEORY

II-1. Background

There are a number of reactor and accelerator-based BNCT facilities around the world. The following is the summary of recent studies.

Argentina

Several studies were performed by Argentinean scientists in collaboration with the Massachusetts Institute of Technology (MIT) Laboratory for Accelerator Beam Applications (LABA). One recent work (Burlon *et al* 2001) investigated the use of the $^{13}C(d,n)^{14}N$ reaction as a neutron source for BNCT. This reaction is one of the most promising deuteron-induced reactions at low incident energy because of the good mechanical and thermal properties of carbon as a target material and carbon has a relatively large neutron production cross-section. The 1.5 MeV deuteron beam used in these studies was produced by an electrostatic tandem accelerator. This high-current accelerator for BNCT was designed for multimilliampere proton or deuteron beams at energies of up to 4.1 MeV. A D_2O moderator and lead reflector assembly was used to provide neutron beam shaping. The dose from the resulting neutron spectrum was evaluated at different depths inside a water-filled brain phantom using the dual ionization chamber technique for fast neutrons and photons and bare and cadmium-covered gold foils for the thermal neutron fluence rate. All results were simulated with the MCNP code. The experimental dose measurements and calculations evaluated at 1,

2, 3, 4, 6, 8, and 10 cm depths on the central axis of the phantom. The treatment time was calculated to be 56 minutes at the depth of 5.6 cm assuming a 4 mA deuteron current.

The same authors recently proposed a design for an optimized neutron-beam shaping assembly for accelerator-based BNCT (Burlon *et al* 2004). They proposed a Li-metal target based on the ^{7}Li(p,n)^{7}Be reaction to produce neutrons. The bombarding proton energies covering the range from 1.92 to 2.5 MeV were used for calculations. A proton energy of 2.3 MeV has some advantages because of the relatively high neutron yield at this energy, which limits the fast neutron dose to healthy tissue and minimizes the treatment times. The beam shaping assembly proposed in this work consists of successive stacks of aluminum, polytetrafluoroethylene (Teflon), and LiF as moderators and neutron absorbers, and lead as a reflector. Lead was used as reflector material in their previous work (Burlon *et al* 2001) and it was shown to be a better than graphite. This assembly is easy to build and relatively inexpensive compared to the widely used Fluental moderator. Three moderator thicknesses were considered (18, 26 and 34 cm) and a 34 cm moderator gave the best performance.

Australia

Australian researchers explored the "near threshold" reaction for the ^{7}Li(p,n)^{7}Be reaction for use in BNCT (Zimin *et al* 2000). The ^{7}Li(p,n)^{7}Be reaction has a proton energy threshold of 1.881 MeV and is used in many studies as a source of nearly monoenergetic neutrons. The maximum achievable epithermal neutron fluence rate on the surface of the phantom was shown to be about $8x10^{7}$ n/cm^{2}-s/mA in the 1.89 – 1.95

MeV proton energy range. Increasing the proton energy in this range has a little benefit because the increase in useful neutron fluence rate is relatively small. Thus, the concept of near-threshold BNCT is feasible only with very high proton beam currents, on the order of 10-20 mA.

Italy

Accelerator-based BNCT has also been studied in Italy. One of the researchers (Bisceglie *et al* 2000) investigated the optimal energy of epithermal neutron beams for BNCT. The results of the simulations, performed for monoenergetic neutron beams over a wide energy range, were analyzed to find the optimal neutron energy for deep-seated tumors. Based on these simulations different accelerator-based neutron-production reactions and beam-shaping assembly configurations were compared.

The most recent Italian work (Terlizzi *et al* 2004) includes a study of Radio Frequency Quadrupole (RFQ) accelerators as an epithermal neutron source for BNCT. A high intensity RFQ accelerator is under construction in Italy as a part of the TRASCO project that includes design of an Accelerator Driven System (ADS) for nuclear waste transmutation. This facility will be able, on one hand, to accelerate a 10 mA proton beam up to 20 MeV for nuclear studies and, on the other hand, to accelerate a 30 mA proton beam up to 5 MeV for BNCT studies. Terlizzi *et al* 2004 also considered a second current regime with proton energies at 2 MeV. Such an accelerator could be used with a $^{7}Li(p,n)^{7}Be$ target to produce neutron beams. An appropriate choice of the function parameters of the RFQ (modulation, efficiency of acceleration, phase shift, etc…) allows

relatively compact accelerators, which could eventually lead to hospital-based BNCT facilities.

Japan

Japan has made a huge scientific contribution in the study of BNCT. Some studies done in Japan in recent years deal with accelerator-based BNCT. Researchers (Tanaka *et al* 2001) investigated the feasibility of neutron capture therapy using an accelerator-based neutron source with the $^{7}Li(p,n)^{7}Be$ reaction produced by 2.5 MeV protons. The neutron beam produced by the Hiroshima University radiological research accelerator (HIRRAC) and the heavy water neutron irradiation facility in the Kyoto University reactor (KUR-HWNIF) were compared with respect to contamination dose ratios for fast neutrons and gamma rays. These contamination ratios to the boron dose were estimated in a water phantom 20 cm in diameter and 20 cm in length to simulate a human head. The $^{7}Li(p,n)^{7}Be$ neutrons produced by 2.5 MeV protons combined with 20-, 25- or 30-cm thick D_2O moderators 20 cm in diameter produced irradiation fields for neutron capture therapy with depth–dose characteristics similar to those from the epithermal neutron beam at the KUR-HWNIF. Tanaka *et al* 2002 also confirmed the feasibility of using a near-threshold $^{7}Li(p,n)^{7}Be$ neutron source for BNCT.

A recent study (Yonai *et al* 2003) at the Cyclotron and Radioisotope Center of Tonoku University focuses on optimizing the epithermal neutron field with an energy spectrum and intensity suitable for BNCT for various combinations of neutron-producing reactions and moderator materials. A thick Ta target was selected as a neutron source, based on the measurement of angular distribution and neutron energy spectra.

All calculations were made using the MCNPX code. This target was simulated as bombarded by 50 MeV protons in a 300 μA beam current and neutrons emitted at 90 degrees from the target. A moderating and shaping assembly used in that simulation was composed of iron, AlF_3, Al, ^6LiF and lead. The depth dose distributions in a cylindrical phantom showed that, for 1 hour or less of therapeutic time, the best moderator assembly, which is 30 cm thick iron, 39 cm thick AlF_3-Al-^6LiF and 1 cm thick lead, provides an epithermal neutron fluence rate of $0.7x10^9$ n/cm^2-s. This results in a tumor dose of 20.9 RBEGy at a depth of 8 cm in the phantom.

This simulation was followed by another study (Yonai *et al* 2004) which was done to validate these calculations. The epithermal neutron energy spectrum passing through the moderators was measured using a ^3He gas spectrometer covered with silicon rubber loaded with natural boron and polyethylene moderator. The depth distribution of the reaction rates was obtained using gold foils in an acrylic phantom set behind the rear surface of the moderators. The measured results were compared with the calculations using MCNPX code. Agreement between the calculations and measurement was to within 10% for the neutron energy spectra and to within 20% for the depth distribution.

Russia

Russian researchers proposed using a proton accelerator complex for fast neutron therapy and for neutron-capture therapy in Russia several years ago (Bayanov *et al* 1998). This project was based on experience accumulated at the Institute of Physics and Power Engineering (IPPE) and the Budker Institute of Nuclear Physics (BINP). The Russians developed an electrostatic accelerator tandem without accelerator columns –

usually an integral part of accepted accelerator scheme. This specific geometry of accelerating electrodes and tandem optics allows maximum reliability in acceleration of high-current proton beams in a continuous mode and a reliable gaseous target can be used for continuous operation. The main components and technical decisions for tandem construction were tested on a 1 MeV prototype which operated in the pulse mode as an H-ion source injector in a synchrotron. Wide experience has been accumulated at BINP in design of negative ion sources of different types. A high power H-continuous ion source with a 40 mA current can be used with lithium neutron-producing target. Liquid lithium targets are necessary to operate with this 100 kW proton beam. For vertical beams a thin lithium layer on the surface of a tungsten disk cooled by a liquid metal is proposed, and a flat liquid lithium jet flowing through the narrow nozzle is proposed for a horizontal beam.

One recent investigation (Kononov *et al* 2004) performed at IPPE in collaboration with Lawrence Berkley National Laboratory and Idaho National Engineering and Environmental Laboratory was to optimize moderator size for creating epithermal neutron beams for BNCT based on this proton accelerator and the $^{7}Li(p,n)^{7}Be$ reaction as neutron source. Such a neutron source is now under construction on the IPPE high current proton accelerator KG-2.5. The best characteristics are obtained using magnesium fluorine. Studies suggest that the optimal configuration for the beam shaping assembly one made from polytetrafluoroethylene and magnesium fluorine. With such a moderator and a 2.3 MeV, 10 mA proton beam, calculations of in-phantom dose distributions show that the advantage depth is 9 cm. The advantage depth determines the

depth in the phantom for which the tumor just receives more dose than the maximum healthy tissue dose (Kudchadker *et al* 1999). The therapeutic ratio is 6 at 3 cm depth, and the advanced dose rate at 9 centimeters is approximately 1 RBEGy per minute, which means that maximum treatment time will be about 10 minutes.

United Kingdom

Many studies have been done at the University of Birmingham. The Dynamitron accelerator at the University of Birmingham has the potential to be the first clinical accelerator-based BNCT facility in the world. The accelerator has demonstrated proton currents in excess of 1 mA at a potential of 2.8 MV. The proton beam strikes a thick natural lithium target positioned at the center of a moderating structure, generating a neutron source intensity of 1.37×10^{12} n/s from the $^{7}Li(p,n)^{7}Be$ reaction. There were a number of studies considering this type of neutron source. A part of this research was analysis of the best proton energy and design for an epithermal neutron beam. A review of some of these works follows.

The first paper (Allen *et al* 1995) described a design concept for an accelerator-based epithermal neutron beam for BNCT. The proposed design was suited to the University of Birmingham's modified Dynamitron accelerator that can deliver a 5 mA vertical proton beam with an energy up to 3 MeV. The facility design concept includes several features. One capability is using a 5 mA beam producing an epithermal neutron therapy beam with a neutron fluence rate of 5×10^{12} n/cm^2-s with low gamma-ray contamination. A thick natural lithium target was used to generate neutrons through the $^{7}Li(p,n)^{7}Be$ reaction. Another proposal was to use a ^{6}Li-poisoned heavy water moderator

to produce a therapy beam with the desired energy spectrum. The neutron fluence rate is maximized by using a graphite reflector placed around the sides and at the rear of the moderator. A hemispherically shaped therapy beam exit surface was designed to partially wrap around a patient's head to maximize the delivery of therapeutic neutrons. The design performance described above has been validated by experiment and, while promising, it suffers some limitations. The most significant was the difficulty in extracting a neutron beam vertically from the Dynamitron accelerator, which has a vertical proton beam. Also some restrictions exist on practical patient positioning and several safety issues remain regarding positioning the proton beam and lithium target directly above a patient.

Thus, another study was conducted (Allen *et al* 1999) to explore further design options available to produce a horizontal neutron therapy beam using the vertical proton beam. A $^{7}Li(n,p)^{7}Be$ thick natural lithium target was used. This target produces a distribution of neutrons peaked in intensity in the direction of the incident proton beam. The neutron fluence rate is expected to decrease gradually at angles away from the forward direction. Furthermore, the mean energy of the emitted neutrons also decreases with increasing angle, so less moderating material could be used. The selected proton energy for that study was 2.8 MeV. Finally, the authors concluded that it was unnecessary to use a collinear neutron beam; a beam extracted at 90 degrees to the direction of the incoming protons produces a better result in terms of lower mean neutron energy at the therapy position. This lower energy improves the achievable therapeutic ratios within a head phantom; the ratios are higher at all depths for an

orthogonal beam delivering the same therapy neutron fluence. The expected treatment time with the proposed 5 mA orthogonal Birmingham facility is of the order of 19 - 40 minutes to deliver a maximum healthy tissue photon equivalent dose of 12.6 RBEGy.

Other research (Allen *et al* 2000) considered the best proton energy for accelerator-based BNCT using the $^{7}Li(p,n)^{7}Be$ reaction and the following proton energies: 2.15, 2.25, 2.4, 2.8, 3.1 and 3.5 MeV. The neutron yield from a thick natural lithium target was calculated as a function of angle and energy at each listed proton energy. The calculated neutron yields were used as the source term in a series of neutron and coupled neutron-photon Monte Carlo simulations using the general purpose code MCNP. This code simulated the transport of neutrons and neutron-generated photons through target, moderator, reflector, shield and phantom. The moderator material chosen, Fluental^{TM}, consists of aluminum, fluorine and natural lithium. Various thicknesses of moderator were studied and the individual dose components were calculated as a function of depth in the phantom. The moderator design was optimized using in-phantom treatment figures of merit, as well as the beam quality. They concluded, that at proton energies below 2.8 MeV, there is no observed variation in the achievable therapy beam quality; but a price is paid in terms of treatment time by not choosing the upper limit of this range. For higher proton energies, the beam quality falls with no improvements in treatment time for optimum configuration.

Another study (Mason *et al* 2001) using the Birmingham BNCT Facility investigated the dependence of the resulting neutron beam on the proton energy and the thickness of moderating material. MCNP was used to explore the extent of this

dependence and the corresponding dose rates in a water-filled polyethylene phantom. The variation in the mean in-phantom neutron energy that can be achieved with an accelerator-based neutron source was analyzed. With a 320 mm moderator, the mean neutron energy was shown to vary from 4.18 keV at a depth of 20 mm to 0.019 keV at a depth of 65 mm for proton energies of 3.5 and 2.15 MeV, respectively. Changing the energy of the proton beam produced the greatest variation, while the thickness of moderating material seems to have a lesser effect. The mean neutron energy varied most at greater depths in the phantom. An irradiation time on the order of several hours was needed to deliver the required dose.

A more recent study at the Birmingham facility was conducted in November 2003 (Culbertson *et al* 2004), analyzing the final epithermal beam design for the BNCT facility constructed at the University of Birmingham. The final moderator and facility design includes a region of Fluental to moderate the neutron spectrum to appropriate therapy energies, with a graphite reflector, and a Li-polyethylene sheet to provide a delimited neutron beam port. A schematic of the system is shown in Figure II-1.

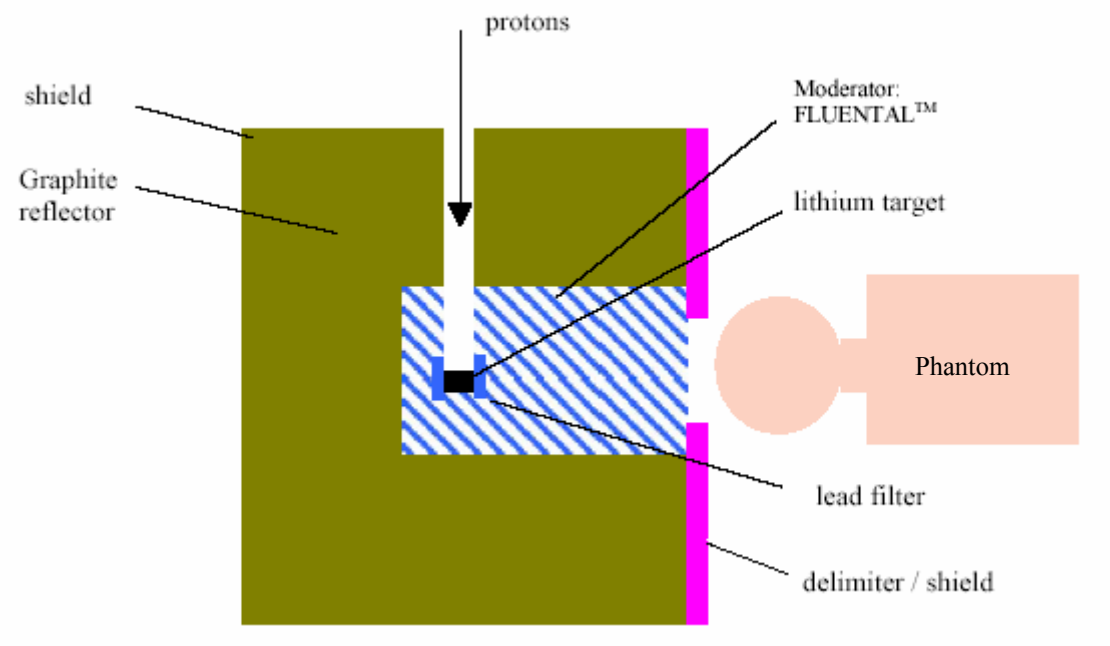

Figure II-1. Current facility design at the University of Birmingham.

The dual ionization chamber technique was used together with foil activation to quantify the fast neutron, photon, and thermal neutron beam dose components in a large rectangular phantom exposed to the beam with a 12-cm diameter beam delimiter in place. The dosimetric characteristics of the Birmingham BNCT facility when measured indicated adequate agreement with in-phantom MCNP predictions, within 10% for the photon and thermal neutron dose, and within 25% for the proton recoil dose along the main beam axis.

United States

Many studies have been done in USA, mostly at Lawrence Berkeley Laboratory, focused on the accelerator-based neutron sources for BNCT. One proposed approach is to use a DC electrostatic quadrupole (ESQ) accelerator to deliver more than 100 mA

beam of 2.5 MeV protons onto a lithium target (Anderson *et al* 1994, Kwan *et al* 1995). Such a high beam current can reduce treatment time to less than an hour and also has an additional advantage of allowing the use of refractory lithium target material to withstand the intense power load. Beam current of more than 100 mA can only be achieved by electrostatic accelerators. But, at present, the critical path lies in the development of a compact, high current, multi-megavolt, DC power supply.

In other research (Bleuel *et al* 1998) the $^{7}Li(p,n)^{7}Be$ reaction was again investigated as an accelerator-driven neutron source for proton energies between 2.1 and 2.6 MeV. Epithermal neutron beams shaped by three moderator materials – Al-AlF_3, ^{7}LiF, and D_2O, were analyzed and their usefulness for boron neutron capture therapy treatments evaluated. The MCNP code was used to simulate radiation transport through the moderator. Fluence and dose distributions in a head phantom were calculated using BNCT treatment planning software. The treatment time was estimated to be about 40 minutes for a single beam treatment, using a 20 mA proton beam and a ^{7}LiF moderator. The tumor dose deposited at a depth of 8 cm was calculated to be about 21 RBEGy. This research was followed by an experimental study (Bleuel *et al* 1999) at the Lawrence Berkeley National Laboratory's 88-inch cyclotron. The epithermal neutron beams, created by using several microamperes of 2.5 MeV protons on a lithium target, were characterized. The neutron moderating assembly consisted of Al-AlF_3 and Teflon, with a lead reflector to produce an epithermal spectrum strongly peaked at 10 – 20 keV. Gold foil activation analysis was used to measure the thermal fluence rate in a cubic lucite head phantom. Portions of the neutron spectrum were measured by in-air activation of

six cadmium-covered materials (Au, Mn, In, Cu, Co, W) with high epithermal neutron absorption resonances. The results agreed reasonably with the Monte Carlo computational models, confirming their validity.

II-2. Monte Carlo code

There are several Monte Carlo codes that are used in medical physics calculations. In this work a general-purpose Monte Carlo N – Particle (MCNP) code was used (Briermeister 2000). This code can be used for neutron, photon, electron, or coupled neutron/photon/electron transport. All calculations have been done in two transport modes: combined neutron/photon transport, where the photons are produced by neutron interactions, and photons only. These transport modes are discussed later. The neutron energy regime is from 10^{-11} MeV to 20 MeV for all nuclides and up to 150 MeV for some nuclides, the photon energy regime is from 1 keV to 100 GeV.

II-2-1. Neutron/photon transport

When simulating a particle collision with a nucleus a series of probabilities and simulation choices have to be made. The following discussion describes this sequence.

II-2-1-1. Identification of the collision nuclide

If there are n different nuclides forming the material in which a collision occurred, and if ξ is a random number on the unit interval [0,1), then the k^{th} nuclide is chosen as the collision nuclide if

$$\sum_{i=1}^{k-1} \Sigma_{ti} < \xi \sum_{i=1}^{n} \Sigma_{ti} \leq \sum_{i=1}^{k} \Sigma_{ti} \quad (1)$$

where Σ_{ti} is the macroscopic total cross-section for nuclide *i*.

II-2-1-2. Free gas thermal treatment

Either the S(α,β) thermal scattering treatment, which is a complete representation of thermal neutron scattering by molecules and crystalline solids, or the velocity of the target nucleus is sampled for low – energy neutrons. This treatment is necessary to account for the thermal motion of the atom and/or the presence of other atoms near the collision site. MCNP uses a thermal treatment based on the free gas approximation to account for the thermal motion. It also has a S(α,β) capability that takes into account the effects of chemical binding and crystal structure for reactions with incident neutron energies below about 4 eV. The free gas thermal treatment consists of adjusting the elastic cross-section and taking into account the velocity of the target nucleus when the kinematics of a collision are being calculated.

II-2-1-3. Optional generation of photons

Photons are generated if the problem is running in the neutron/photon transport mode and if the collision nuclide has a nonzero photon production cross-section. Any photons generated at neutron collision sites are temporarily stored in the bank. There are two different methods to determine photon energies and directions.

The first method is the Expanded Photon Production Method. In this method, the reaction *n* responsible for producing the photon is sampled from

$$\sum_{i=1}^{n-1}\sigma_i < \xi\sum_{i=1}^{N}\sigma_i \le \sum_{i=1}^{n}\sigma_i \tag{2}$$

where ξ is a random number on the interval (0,1), *N* is the number of photon production reactions, and σ_i is the photon production cross-section for reaction *i* at the incident neutron energy. Every neutron reaction has associated energy-dependent angular and energy distributions for the secondary neutrons. Moreover, every photon reaction has associated energy-dependent angular and energy distributions for the secondary photons.

The second method is the "30x20" Photon Production Method. This method uses photon production data contained in older libraries. In contrast to the expended photon production data, the only secondary photon data used are a 30x20 matrix of photon energies; that is, for each of 30 incident neutron energy groups there are 20 equally probable photon energies.

II-2-1-4. Modeling of the neutron capture

There are two ways of treating capture: analog and implicit.

In analog capture, the particle is killed with probability σ_a/σ_T, where σ_a and σ_T are the absorption and total cross-sections of the collision nuclide for the incoming neutron energy. MCNP defines the absorption cross-section as the sum of all *(n,x)* cross-sections, where *x* is anything except neutrons. For all particles killed by analog capture, the entire particle energy and weight are deposited in the collision cell.

The default method of neutron capture used by MCNP is the implicit capture. For that capture, the neutron weight W_n is reduced to W_n' as follows:

$$W_n' = \left(1 - \frac{\sigma_a}{\sigma_T}\right) * W_n \tag{3}$$

For implicit capture, a fraction σ_a/σ_T of the incident particle weight and energy is deposited in the collision cell corresponding to that portion of the time that the particle is captured.

II-2-1-5. Elastic and inelastic scattering

The selection of an elastic collision is made with probability

$$\frac{\sigma_{el}}{\sigma_{in} + \sigma_{el}} = \frac{\sigma_{el}}{\sigma_T - \sigma_a} \tag{4}$$

where σ_{el} is the elastic scattering cross-section.

σ_{in} is the inelastic cross-section.

σ_a is the absorption cross-section.

σ_T is the total cross-section, $\sigma_T = \sigma_{el} + \sigma_{in} + \sigma_a$.

The selection of an inelastic collision is made with probability

$$\frac{\sigma_{in}}{\sigma_T - \sigma_a} \tag{5}$$

The type of inelastic reaction, *n*, which includes any neutron out process – *(n,n'), (n,f), (n,np)*, etc., is sampled from

$$\sum_{i=1}^{n-1} \sigma_i < \xi \sum_{i=1}^{N} \sigma_i \leq \sum_{i=1}^{n} \sigma_i \tag{6}$$

where ξ is a random number on the interval [0,1), N is the number of inelastic interactions, and the σ_i's are the inelastic reaction cross-sections for the incident neutron energy. For both elastic and inelastic scattering, the direction of exiting particles usually is determined by sampling angular distribution tables from the cross-section files.

II-2-1-6. S(α,β) treatment

If the neutron energy is low enough and an appropriate S(α,β) table is available, the collision is modeled by the S(α,β) treatment instead of by step *II-2-1-5*, which describes elastic and inelastic scattering. During this treatment the zero-temperature elastic cross-section is adjusted to account for the thermal motion of the atom. The elastic scattering treatment is chosen with probability $\sigma_{el}/(\sigma_{el}+\sigma_{in})$. The S(α,β) thermal scattering treatment also allows the representation of scattering by multiatomic molecules. For inelastic scattering, the distribution of secondary energies is represented by a set of equally probable final energies for each member of a grid of initial energies from an upper limit of typically 4 eV down to 10^{-5} eV. Also, there is a set of angular data, which corresponds to each initial and final energy.

II-2-2. Photon interactions

Sampling of the collision nuclide, analog capture, implicit capture, and other aspects of photon interactions is the same as for neutrons. But the collision physics is completely different. There are two photon transport models used by MCNP: simple and detailed.

The first is the simple treatment method. This method ignores coherent (Thomson) scattering and fluorescent photons from photoelectric absorption. It is intended for high-energy photon problems or problems where electron binding effects may be neglected.

Usually, the default method for photon transport in MCNP is the detailed physics method. This method includes coherent (Thomson) scattering and accounts for fluorescent photons after photoelectric absorption. Form factors are used with coherent and incoherent scattering to account for electron binding effects.

II-2-3. Tallies

MCNP provides seven standard neutron tallies, six standard photon tallies, and four standard electron tallies. All tallies are normalized to be per starting particle. The F4 tally which represents the average fluence in a cell has been used in this research. Another name for the F4 tally is Track Length Estimate of Cell Fluence rate. The definition of particle fluence rate is $\Phi(\vec{r},E,t)=vN(\vec{r},E,t)$, where v is a particle velocity, N is a particle density or particle weight/unit volume. Roughly speaking, the time integrated fluence rate is

$$\int_V \int_t \int_E \Phi(\vec{r},E,t)dEdt\frac{dV}{V} = Wtv/V = WT_l/V \tag{7}$$

where W is a particle weight.

T_l is a track length (cm) = transit time*velocity.

V is a volume (cm^3).

More precisely, let $ds=vdt$. Then the time-integrated fluence rate is

$$\int_V \int_E \int_t \Phi(\vec{r}, E, t) dt dE \frac{dV}{V} = \int_V \int_E \int_s N(\vec{r}, E, t) ds dE \frac{dV}{V} \quad (8)$$

Because $N(\vec{r}, E, t)\, ds$ is a track length density, this integral is estimated by summing WT_l/V for all particle tracks in the cell, time range, and energy range. This tally is generally quite reliable because there are frequently many tracks in a cell (compared to the number of collisions), leading to many contributions to this tally.

In this research the resulting tallies are multiplied, using FM tally multiplier, by the Neutron Fluence Rate-to-Dose Rate Conversion Factors given in Tables II-1 and II-2. These conversion factors convert the average fluence rate in the cell to the biological dose equivalent rate.

Table II-1. Neutron fluence rate-to-dose rate conversion factors (ICRP-21).

Energy, MeV	DF(E), (rem/hr)/(n/cm^2-s)
2.5E-08	3.85E-06
1.0E-07	4.17E-06
1.0E-06	4.55E-06
1.0E-05	4.35E-06
1.0E-04	4.17E-06
1.0E-03	3.70E-06
1.0E-02	3.57E-06
1.0E-01	2.08E-05
5.0E-01	7.14E-05
1.0	1.18E-04
2.0	1.43E-04
5.0	1.47E-04
10.0	1.47E-04
20.0	1.54E-04

Table II-2. Photon fluence rate-to-dose rate conversion factors (ICRP-21).

Energy, MeV	DF(E), (rem/hr)/p/cm^2-s)
0.01	2.78E-06
0.015	1.11E-06
0.02	5.88E-07
0.03	2.56E-07
0.04	1.56E-07
0.05	1.20E-07
0.06	1.11E-07
0.08	1.20E-07
0.1	1.47E-07
0.15	2.38E-07
0.2	3.45E-07
0.3	5.56E-07
0.4	7.69E-07
0.5	9.09E-07
0.6	1.14E-06
0.8	1.47E-06
1	1.79E-06
1.5	2.44E-06
2	3.03E-06
3	4.00E-06
4	4.76E-06
5	5.56E-06
6	6.25E-06
8	7.69E-06
10	9.09E-06

II – 3 GE PETtrace cyclotron

This research investigates the possibility of making BNCT available for clinics and research groups that do not have a specially designed BNCT nuclear reactor or an accelerator. There are a large number of medical cyclotrons used for medical radionuclide production in the nuclear pharmacies and hospitals. These cyclotrons are designed mostly for fluorodeoxyglucose (FDG) production. FDG is manufactured in an automated synthesis unit from ^{18}F. This nuclide is produced in a cyclotron by proton bombardment of enriched water (^{18}O).

In this research the General Electric (GE) PETtrace cyclotron normally used to produce FDG is examined for use in BNCT (Figure II-2).

The GE PETtrace was chosen for this investigation because this type of cyclotron is popular among nuclear pharmacies and clinics in many countries (about 75 PETtraces have been sold world wide); it's compact and reliable; it produces protons with energies large enough to produce neutrons with appropriate energy and fluence rate for BNCT and it does not require significant changes in design to provide neutrons suitable for BNCT. The energy of protons made in this cyclotron is fixed at 16.5 MeV. The current on the target runs up to 60 μA. Targets are accessible, easily changeable, and this cyclotron can use dual targets simultaneously, so it gives flexibility to work on radionuclide production and BNCT with minimal investment of time and workforce. Following is the overview of some design features of the GE PETtrace cyclotron.

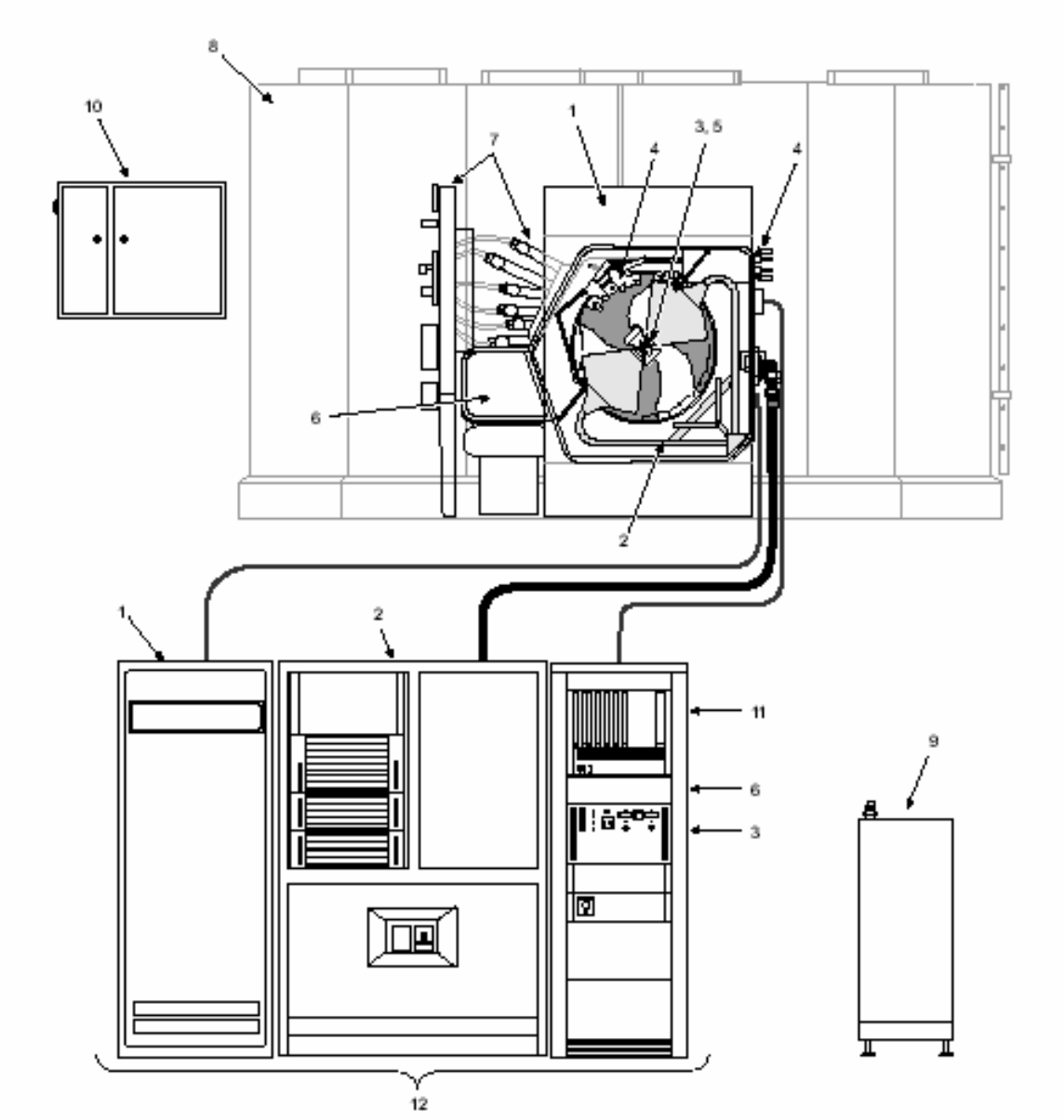

Figure II-2. The accelerator (adapted from the PETtrace Reference Manual (GE Medical Systems 2000)).1 – Magnet System; 2 – Radio-Frequency (RF) System; 3 – Ion Source System; 4 – Beam Extraction System; 5 – Beam Diagnostic System; 6 – Vacuum System; 7 – Target System; 8 – Radiation Shield (option); 9 – Secondary Water Cooling System; 10 – Power Distribution System; 11 – Accelerator Control Unit; 12 – Electronics and Power Supplies

The cyclotron consists of a large cylindrical chamber, placed between the poles of a large electromagnet (GE Medical Systems 2000). The cyclotron is used for accelerating charged particles (hydrogen ions H^- or deuterium ions D^- ions). In this research, the ability of the cyclotron to accelerate hydrogen ions is used. The chamber is evacuated until a very high vacuum exists and H^- ions are fed into the center of the chamber by means of an ion source. The chamber contains two hollow, D-shaped electrodes, called dees, which are connected to a source of very high voltage, oscillating with high frequency. When the cyclotron is in operation, the electric charge on these dees is reversed very rapidly following the high frequency input voltage. The electromagnetic field in conjunction with the high voltage alternating potential causes the H^- ions inside to take a spiral course. They move faster and faster and acquire more and more energy. The H^- ions are transformed to protons after reaching the outer rim of the chamber and then deflected toward a target. The PETtrace has up to six targets mounted on a flange at the front of the cyclotron (Figure II-3).

Modifying this cyclotron for BNCT presents a number of difficulties:

-there is no known target for BNCT, so this will require research for a new target system;

-positioning of some cyclotron equipment (behind the targets) will scatter neutrons emitted in the forward direction and could result in less fluence rate than required by BNCT, so the system configuration might have to be changed;

-some of these cyclotrons are assembled as self-shielded units (stainless tanks filled with borated water surround the cyclotron), and this configuration makes it

impossible for them to serve as a neutron source.

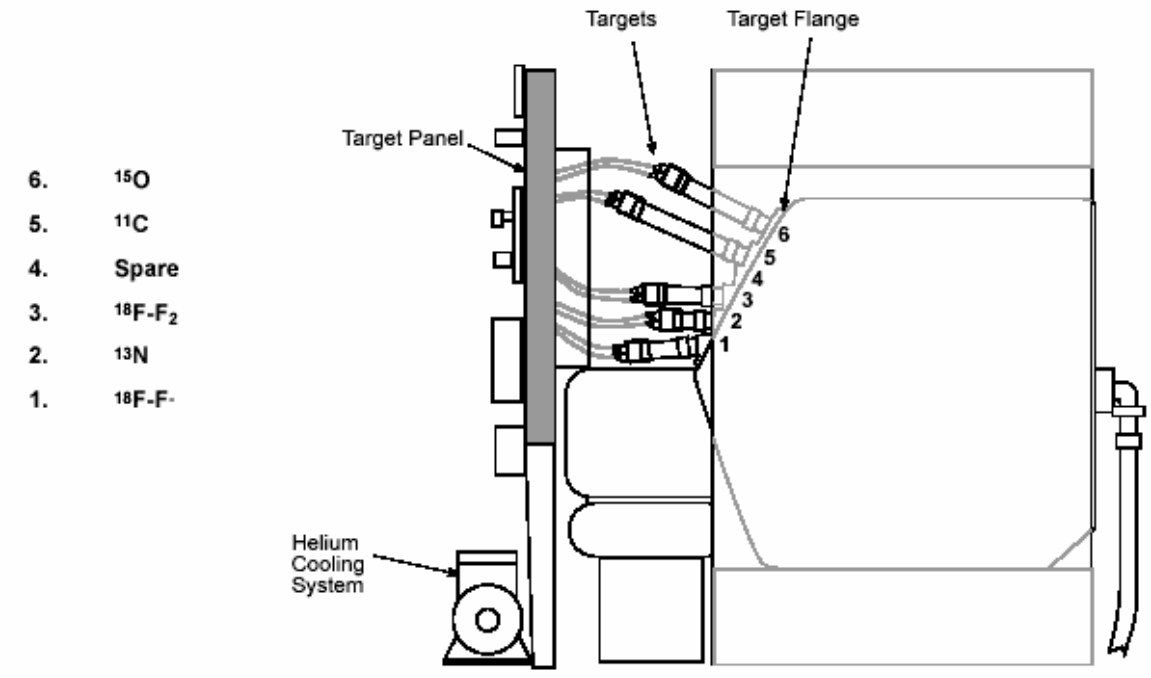

Figure II-3. Target system, standard configuration (adapted from the PETtrace Reference Manual (GE Medical Systems 2000)).

Considering these advantages and disadvantages of GE PETtrace, calculations were conducted to study the possibility of using an ^{18}O target as a source of neutrons with further reflection, moderation, absorption, and collimation to produce appropriate energy and fluence rate for BNCT.

The ^{18}O target was studied because about 90-95% of time these cyclotrons use this target already for FDG production. The efficiency of cyclotron use may be significantly increased if unused neutrons produced during FDG production could be utilized for other medical modalities such as BNCT at the same time. This research

investigates this source using Monte Carlo techniques and standard neutron data files subject to the following assumptions:

-standard running conditions (60 μA target current, 16.5 MeV protons, standard ^{18}O target);

-no target filler system behind the target;

-cyclotron is in a vault with no self-shielding (Figure II-4).

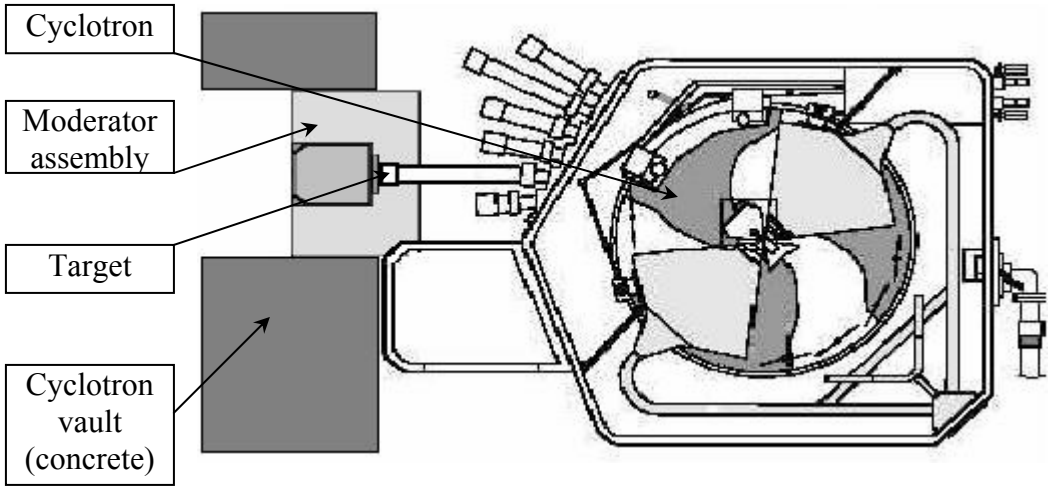

Figure II-4. Cyclotron vault with channel for filters and collimators proposed for BNCT (side view).

CHAPTER III

MONTE CARLO SIMULATIONS

III – I. Geometry

Transport of neutrons was simulated using MCNP. For the initial calculation the geometry shown in Figure III-1 was used.

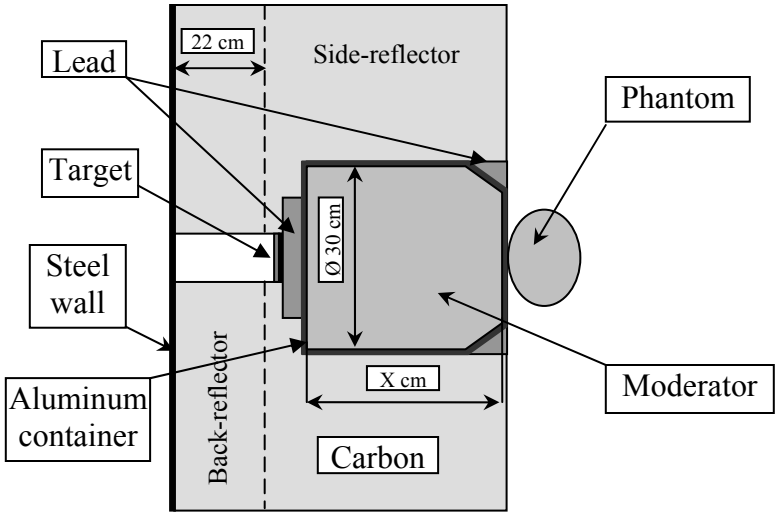

Figure III–1. Geometry defined as input for the MCNP.

III – 1 – 1. Moderator

This geometry includes a moderator assembly surrounded by a thick carbon reflector. The moderator assembly consists of an aluminum container filled with a moderating material. Several different types of materials were investigated to moderate neutrons to the epithermal energies: light water, carbon, heavy water. Another popular type of BNCT moderator – Fluental^{TM} (43.2% Al, 55.9% F and 0.9% Li by weight),

consisting of aluminum, fluorine and natural lithium was also considered (Auterinen *et al* 1993).

It is worth briefly examining the neutron cross sections of different moderating materials. The data were taken from the ENDFB 6.8 cross-section library. As shown in Figures III-2 and III-3, all elements have scattering cross-sections of the same order of magnitude for neutrons having energies between 1 to 10 MeV. Light hydrogen has the highest elastic scattering cross section compared to other elements for neutrons with energy less than 1 MeV. On the other hand, it has large absorption cross-section, especially for low energy neutrons. The magnitude of carbon, fluorine and deuterium scattering cross-sections is about the same; but the absorption cross-section of deuterium is much lower compared to that of carbon and fluorine. One of the major components of Fluental^{TM} – aluminum, has the lowest scattering and highest absorption cross-sections among the other elements. One of the benefits of using Fluental^{TM} as a moderator is that the fluorine and aluminum scattering cross-sections have series of resonances at high energies which provide a good moderation of neutrons down to epithermal energies, where the cross-section is much smaller. A disadvantage of these Fluental^{TM} components, compared to other moderating materials, is that both of them, especially aluminum, are readily activated by neutrons followed by emission of high-energy gammas.

All moderating materials can be compared using a figure of merit called the moderation ratio that depends on three quantities:

1. Σ_s, the scattering cross section for neutrons. Larger is better, because it means that the nuclide is efficient at colliding with neutrons.
2. ξ, the "lethargy decrement". This is the average energy lost by a neutron in a collision with the nuclide. Larger is better, because it means that the neutron is thermalized in fewer collisions.
3. Σ_a, the absorption cross section for neutrons. Smaller is better, because it means that the nuclide is poor at absorbing neutrons.

Moderating ratio $\frac{\xi\Sigma_s}{\Sigma_a}$ is a measure of the efficiency of moderation without absorption.

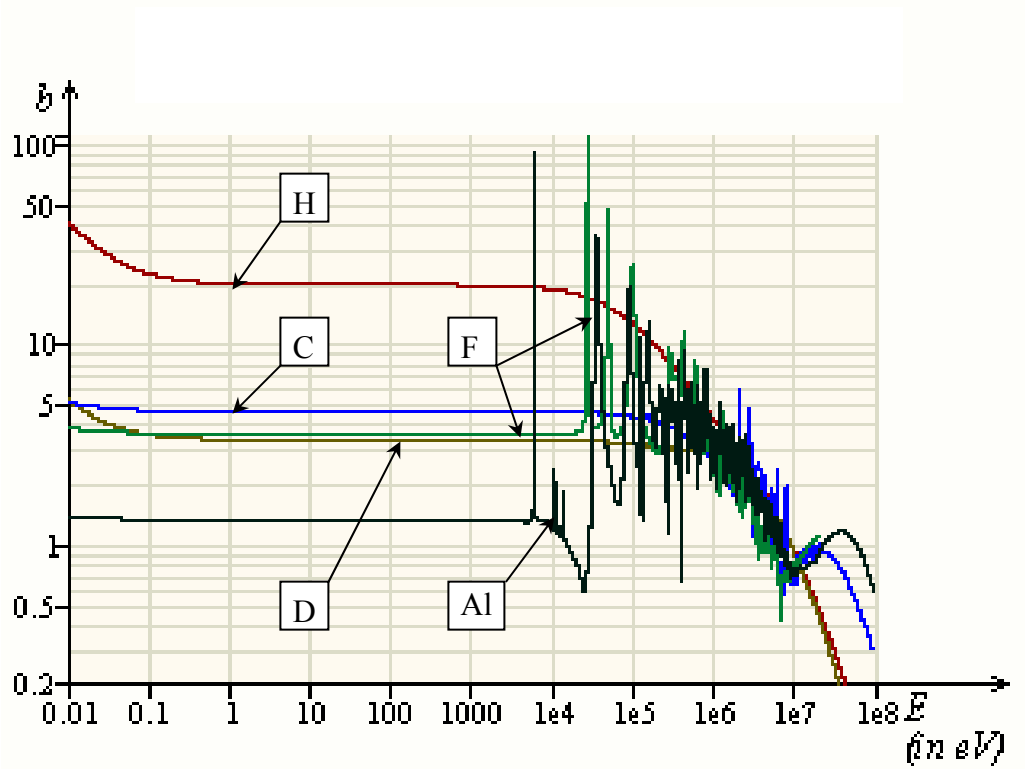

Figure III-2. Elastic cross-sections of moderating materials.

Heavy water is the best moderator, as it has the highest moderating ratio. But other materials were also considered for several reasons. Light water, for example, readily absorbs neutrons but, on the other hand, neutrons can be thermalized with a moderator of much less thickness. This enables positioning of a phantom closer to a neutron source and might compensate the loss of neutrons due to absorption. Using Fluental™ may be beneficial, considering moderation of neutrons with high energies.

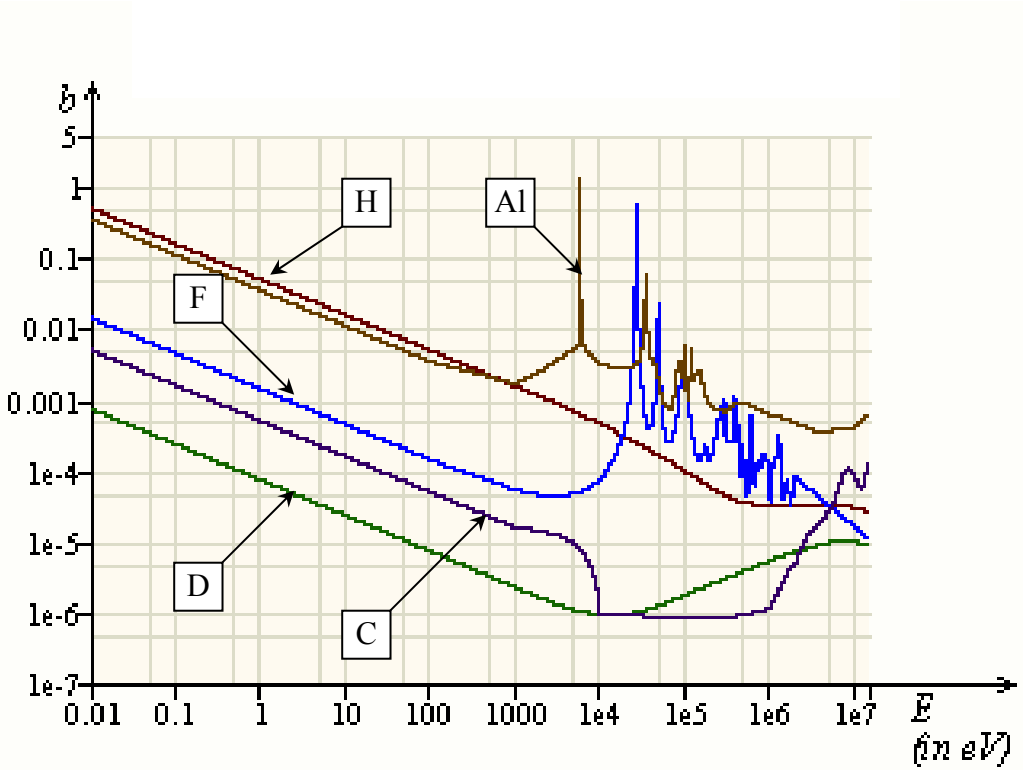

Figure III-3. Absorption cross-sections of moderating materials.

Various thicknesses of moderating material were used in this study, see Table III-1.

Table III-1. Moderator thicknesses used for the MCNP calculations.

	25 cm	30 cm	40 cm	50 cm
H_2O	Y	Y	n/a	n/a
D_2O	Y	Y	Y	Y
Carbon	n/a	Y	Y	n/a
Fluental™	n/a	Y	Y	n/a

The thickness that provided the lowest fast-neutron contribution to the total fluence rate in comparison to the low-energy component and that allowed delivery of the necessary dose in a reasonable time was investigated, see *Chapter III - 4*.

III – 1 – 2. Filter

Different filters can be used to improve the neutron fluence rate properties. The ^{60}Ni isotope, for example, can be very useful as a neutron filter to improve the epithermal to fast neutron ratio in the BNCT neutron beam (Gritzay *et al* 2004). In this research, a 2-cm thick natural nickel filter was analyzed at different positions inside the moderator container. Natural nickel was chosen instead of the pure ^{60}Ni isotope because of the high cost of enrichment. The natural abundance of ^{60}Ni is 26.22% and the other major isotope of nickel is ^{58}Ni, with a natural abundance of 68.08%. Figures III-4 and III-5 show the scattering and the absorption cross-sections for the two nickel isotopes compared with the deuterium cross-sections.

The nickel absorption cross-section is higher than that of heavy water. Thus, the Ni filter should slightly decrease the epithermal neutron fluence rate due to absorption. However, considering the scattering cross-section, it may be that epithermal fluence rate

is increased in the region of 1 – 10 keV. The scattering cross-section of ^{60}Ni has the interference minimum at 5 keV with a width of about 7 keV, reaching 0.0001 b at its minimum, but cross-section in the energy range of 10 – 100 keV increases up to 200 b.

Thus, the use of a Ni filter should allow scattering of the high-energy neutrons and accumulating of these neutrons in the energy range of 1 – 10 keV.

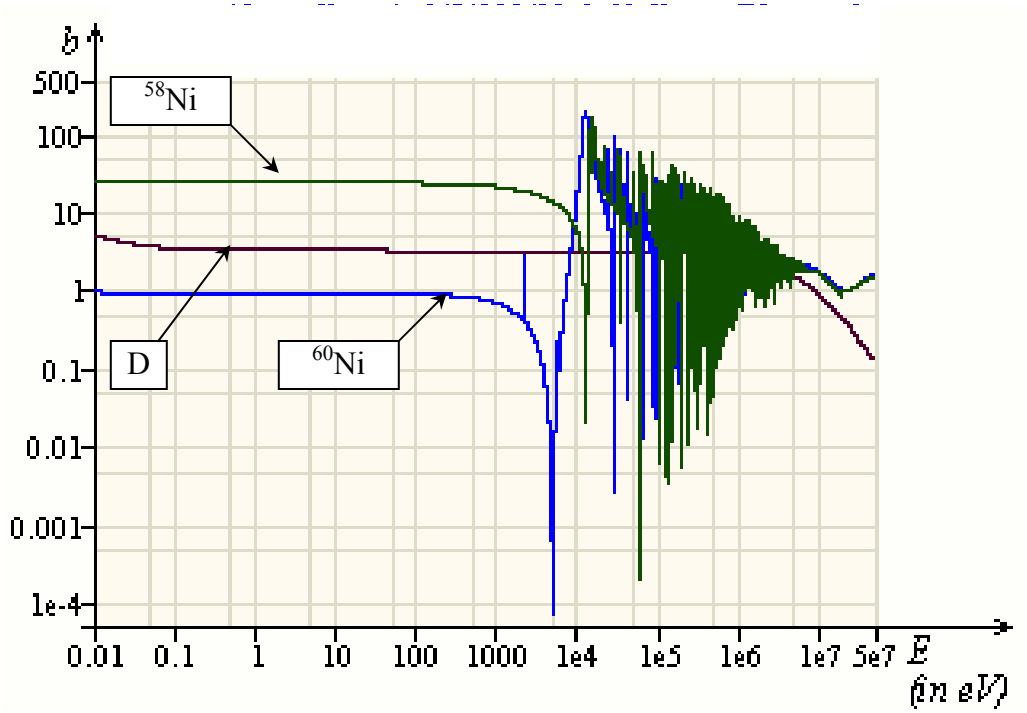

Figure III-4. Scattering cross-sections of filter materials.

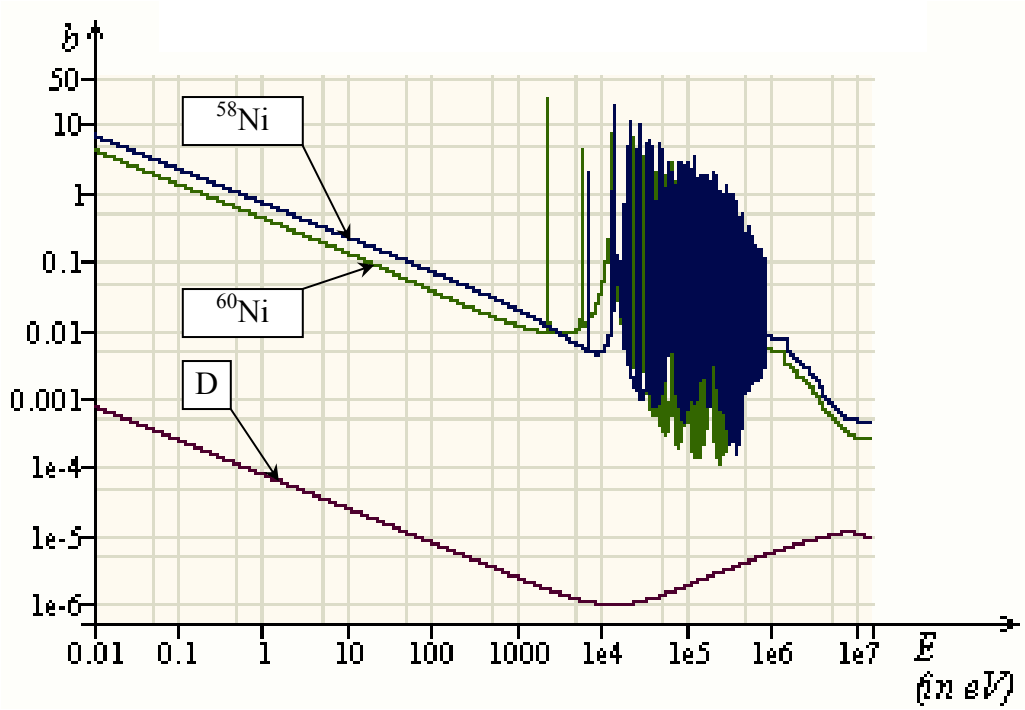

Figure III-5. Absorption cross-sections of filter materials.

III – 1 – 3. Reflector

The proposed reflector consists of two major parts: a side-reflector and a back-reflector. Three materials were considered as possible reflectors: graphite, lead, and aluminum oxide, Al_2O_3. After detailed analysis, graphite was chosen as the reflector material. The reasons for this decision are the following. Aluminum oxide generates many more high-energy photons than graphite and lead when bombarded by neutrons, leading to higher photon dose to a healthy tissue. Lead has a lower moderating power than graphite, therefore, more fast neutrons are reflected from the lead than from the graphite reflector. By itself and by photon induction in the tissues, this higher fast neutron component in the neutron beam provides an additional dose to a healthy tissue. After choosing graphite as the reflector material, the benefits of using a back-reflector

were considered. Scoping calculations using MCNP were carried out for two geometries with and without a 22-cm thick graphite back-reflector. The neutron spectra at 3 cm depth inside a phantom were compared for both geometries, see Figure III-6. A back-reflector almost doubled thermal neutron fluence rate at the 3-cm depth. These calculations assumed a 30-cm thick side-reflector and a 22-cm thick back-reflector. Several studies (Allen *et al* 1995, Allen *et al* 2000 and Bleuel *et al* 1998) considered graphite as a reflector. It has been shown that the graphite thickness should be on the order of 20 – 30 cm to effectively reflect neutrons and there is a little merit in further increasing the graphite thickness. Thus, a 30-cm thick side-reflector and a 22-cm thick back-reflector were used for all further analysis.

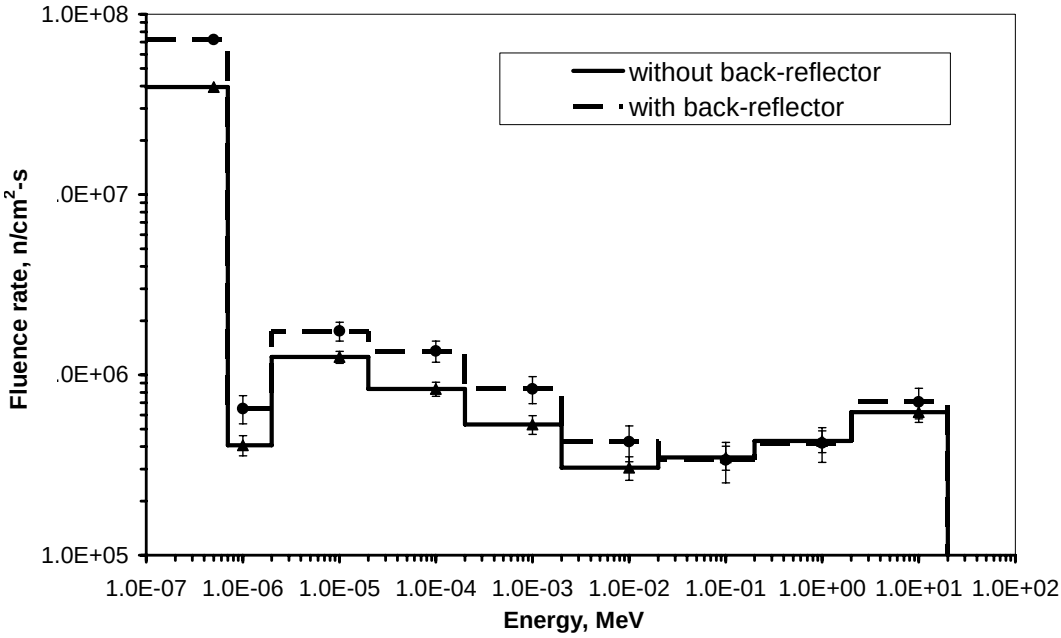

Figure III-6. Neutron spectra for two different geometries.

III – 1 – 4. Phantom

The neutrons emitted from the target slow down through scattering reactions. The neutrons leave the moderator and may then interact within the brain for BNCT treatment. The phantom brain used to model these interactions consists of an ellipsoid with major axies (Harling *et al* 1995) of 13.6, 19.6 and 16.6 cm to represent human head. This phantom was filled with a special composition to simulate brain tissue (ICRU-44 1989) see Table III-2. The tissue density inside the phantom brain was set to 1.04 g/cm^3 (ICRU-44 1989). The skull bone was considered part of the brain phantom and was not defined separately. Bone has approximately the same composition as brain tissue (ICRU-44 1989). It contains approximately half the hydrogen and oxygen weight fractions, but has a higher density of 1.92 g/cm^3 compared to brain tissue, so, basically, it cancels this difference out. Also, bone contains a bit of calcium that is not present in brain, but this element should not affect very much on moderating properties.

The tally cells were 0.5 cm diameter spheres at depths of 1, 2, 3, 4, 5, 6, 7 and 8 cm inside the phantom brain. The fluence rate tally was used in this study to calculate photon and neutron dose, by applying fluence rate-to-dose conversion factors given in Tables II-1 and II-2.

Table III-2. Bone and brain tissue compositions.

Element	Fraction by weight	
	Bone	Brain tissue
Hydrogen	0.034	0.107
Carbon	0.155	0.145
Nitrogen	0.042	0.022
Oxygen	0.435	0.712
Sodium	0.001	0.002
Magnesium	0.002	-
Phosphorus	0.103	0.004
Sulfur	0.002	0.002
Chlorine	-	0.003
Potassium	-	0.003
Calcium	0.225	-

III – 1 – 5. Construction and shielding materials

Construction and shielding materials used in a given geometry include steel walls, a lead shield, container filled with a moderating material, and a lead collimator. A steel wall represents the body of a cyclotron and provides additional neutron back-scattering. A lead block, which is placed next to the target, thickness of 4 cm, is used to reduce the dose from the photons emitted from the target. A lead collimator forms the neutron beam, thus decreasing unwanted irradiation of healthy tissue. The container wall that holds the moderating material consists of aluminum with a thickness of 1 cm for structural considerations.

III – 2. Source

The typical ^{18}O target consists of ^{18}O-enriched water kept under a helium overpressure in a silver container. The enrichment of ^{18}O in the target is not less than 95%. When bombarded with neutrons the following reaction occurs in the target:

$$^{18}_{8}O+^{1}_{1}p\rightarrow^{18}_{9}F+^{1}_{0}n-2.57MeV$$

^{18}F and neutron production in target is well established. The cross-section for this reaction is shown on Figure III-7.

The neutron spectrum and the angular distribution of neutrons have been provided by General Electric (Lundgren and Ingemannson, 2001) and are shown in Figures III-8 and III-9. The total neutron yield from the target is 3.21×10^{11} n/s. As it can be seen from the spectrum, most of the neutrons have energy on the order of a few MeV.

There are several reasons for such a neutron energy distribution.

1. The target is thick for 16.5 MeV protons (the range of 16.5 MeV protons in water is approximately 3 mm). Thus, incident protons are slowing down very fast by scattering reactions. Scattering in water produces additional scattered protons which have much lower energy (half on average) compared to that of incident protons.
2. The (n,p) reaction cross-section for ^{18}O has a maximum for neutrons in the energy range of 3 to 6 MeV. Thus, taking into account the large number of scattered protons in that energy range and the negative Q-value of the reaction, which is equal -2.57 MeV, a large number of 1 to 2 MeV neutrons may be predicted.

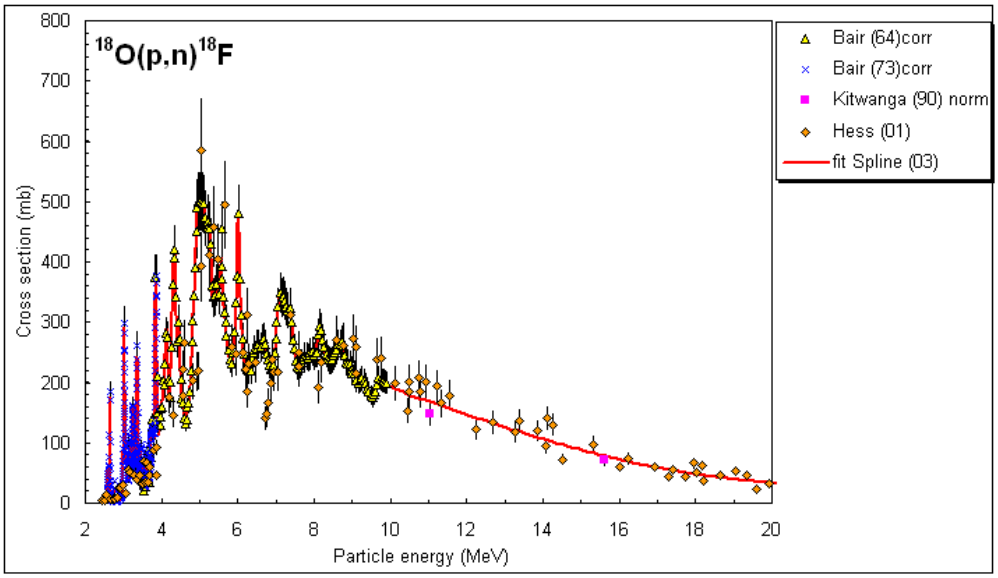

Figure III-7. Cross-sections for the $^{18}O(p,n)^{18}F$ reaction (IAEA 2001).

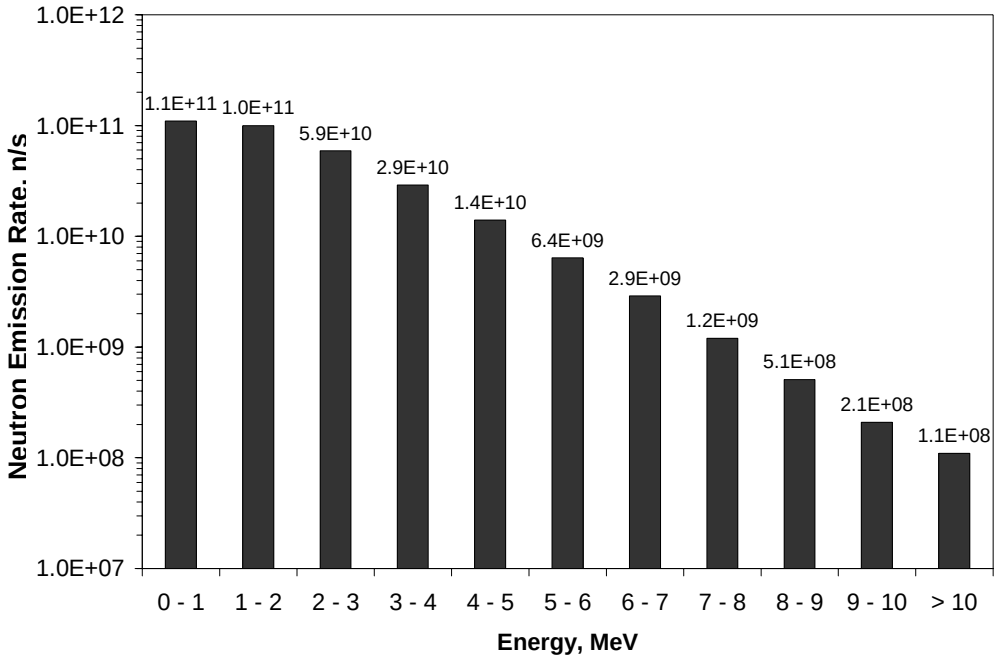

Figure III-8. Neutron spectrum from $H_2{}^{18}O$ target.

This data, along with corresponding neutron yield for different angular directions, were used to define the neutron source in the MCNP calculations. An angular distribution from 0º to 180º with bins covering every 20º was constructed for input.

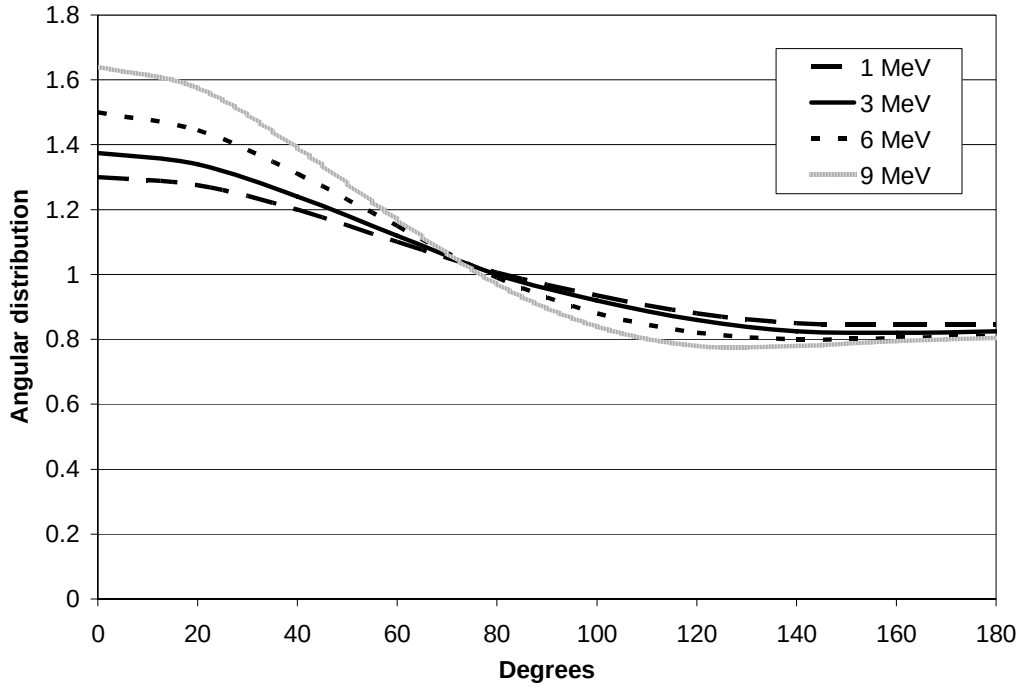

Figure III-9. Neutron angular distribution.

Besides neutrons the target also emits gammas. The gamma spectrum was provided by General Electric (Lundgren and Ingemannson, 2001) and is shown in Figure III-10. Most of the gammas have energy of few MeV and must be shielded to prevent additional damage to healthy tissue.

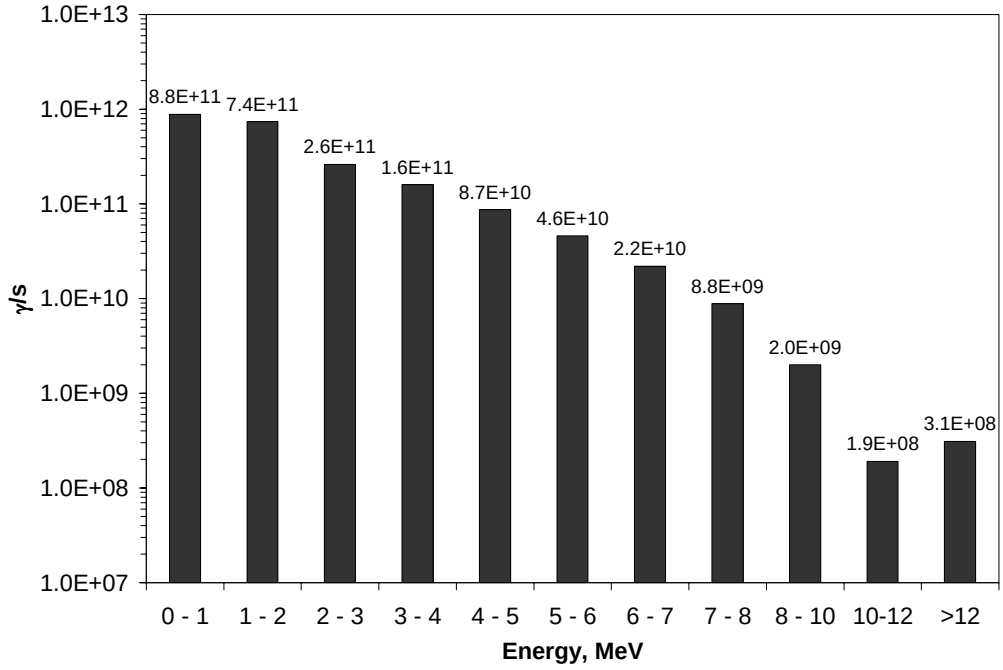

Figure III-10. Gamma spectrum from $H_2{}^{18}O$ target.

The half-value layer of lead, *X,* for 2 MeV neutrons may be calculated using the following formula:

$$X = -\frac{\ln(0.5)}{\mu * \rho}, \text{ cm} \tag{9}$$

where μ – is the mass attenuation coefficient of lead for 2 MeV photons ($4.6 \times 10^{-2} cm^2/g$); and ρ – is the density of lead (11.35 g/cm^3).

The half-value layer of lead obtained using formula (9) is equal 1.3 cm, so 4 cm of lead shield placed in front of the target should reduce the dose from gammas by approximately a factor of 8.

The gamma source was assumed to be isotropic. This assumption, along with the gamma spectrum, was used to specify the gamma source for the MCNP calculations.

III – 3. Input files for MCNP

Two different input files were created for each moderator thickness. The first type contains the anisotropic neutron source with parameters described in *III – 2* and starts the neutron transport calculation for a given geometry. An example of the input file for the neutron dose calculation may be found in APPENDIX A. The other type of input file describes an isotropic gamma source with the spectrum shown on Figure III-10 and initiates a gamma-dose calculation. The input file, shown in the APPENDIX B, gives a gamma-dose calculation at different depths inside the brain phantom. Such input files were used for each of the proposed moderators and different thicknesses. The calculation time for the each geometry was at least one week in order to lower the statistical error of the results.

III – 4. Calculations

Most neutrons have been thermalized at the tally depths. So, in order to know the total dose delivered in the tumor and the healthy tissue, other components of the total dose were calculated. There are two principal capture reactions for thermal neutrons in tissue – $^{1}H(n,\gamma)^{2}H$ and $^{14}N(n,p)^{14}C$ (Turner 1995). The first capture reaction releases a 2.22 MeV gamma ray, that deposits a fraction of its energy before escaping the phantom. In contrast, the nitrogen capture reaction releases 0.626 MeV, which is deposited by the

proton and recoil carbon nucleus in the immediate vicinity of the capture site. The resulting dose rate from exposure to thermal neutrons was calculated using the following formula (10):

$$D_{14N} = \Phi_{th} F_n^{14N} f_{14N} \tag{10}$$

where D_{14N} is the dose rate due to capture in nitrogen (cGy/s), Φ_{th} is the neutron fluence rate(n/cm^2-s), F_n^{14N}=0.785x10^{-9} cGy-cm^2/n is the kerma factor for thermal neutrons, and f_{14N}=0.022 is the weight fraction of nitrogen in brain tissue (Harling *et al* 1995). Kerma factors for this reaction were taken from the literature (Caswell *et al* 1980). In the neutron reaction, ^{10}B(n,γ)^{7}Li, the charged particles are produced with a total kinetic energy of 2.34 MeV on average and with a range in tissue of about 10 μm, the order of the size of a tumor cell. As a result, the cell containing ^{10}B can be effectively destroyed. A similar formula (11) was used to obtain the dose rate from the neutron reaction with ^{10}B.

$$D_{10B} = \Phi_{th} F_n^{10B} \tag{11}$$

where D_{10B} is the dose rate due to capture on boron (cGy/s), Φ_{th} is the neutron fluence rate (n/cm^2-s), F_n^{10B}=8.6x10^{-12} cGy-cm^2/n is the corrected kerma factor for thermal neutrons obtained per 1 ppm concentration of ^{10}B in tissue (Rogus *et al* 1994). The total dose to healthy tissue and to tumor cells was calculated using the following formula:

$$D(RBE)_{tissue} = D(RBE)_{fast} + D(RBE)_{photon} + D_{14N} RBE_{14N} + D_{10B} RBE_{10B} \tag{12}$$

where $D(RBE)_{tissue}$ is the effective dose rate to tissue (RBEcGy/min), $D(RBE)_{fast}$ is the simulated neutron dose rate (RBEcGy/min), $D(RBE)_{photon}$ is the simulated photon dose

rate (RBEcGy/min), D_{14N} and D_{10B} are the dose from interactions of thermal neutrons with nitrogen and boron, and RBE_{14N}=3.2, RBE_{10B}=1.3 (for normal tissue) and RBE_{10B}=3.8 (for tumor) are the relative biological effectiveness given in literature (Coderre *et al* 1993). B-10 concentrations in normal tissue of 11.4 ppm and within the tumor of 40 ppm were assumed (Coderre *et al* 1998).

All the formulae (10 – 12), along with data obtained from the MCNP calculations, were used to evaluate the dose rate for a number of geometries described above in Table III-1.

III – 4 – 1. Results for a light water moderator

Two different thicknesses of light water moderator, 25 and 30 cm, were investigated. As predicted, light water heavily absorbed neutrons. Thus, the resulting neutron fluence rates came out to be very low, see Figure III-11. The desired neutron fluence rate should be on the order of 10^8 – 10^9 n/cm^2-s to provide a reasonable treatment time.

Figure III-12 shows neutron spectra for both moderator thicknesses at 3-cm depth inside the brain phantom. Calculation results for each dose component, using formulae (2 – 4), are presented in Tables III-3 and III-4. The fast-to-thermal neutron ratio is about the same for both geometries, providing approximately the same therapeutic ratios, i.e. ratio of the tumor dose to that of healthy tissue, for different moderator thicknesses. Since the neutron fluence rate is very low, the boron capture provides only a little contribution to the total dose. Thus, the therapeutic ratio, which is mainly dependent on

the dose component coming from the neutron capture in boron, is close to 1. That means a light water moderator is not beneficial and cannot be a part of the irradiation system used for BNCT.

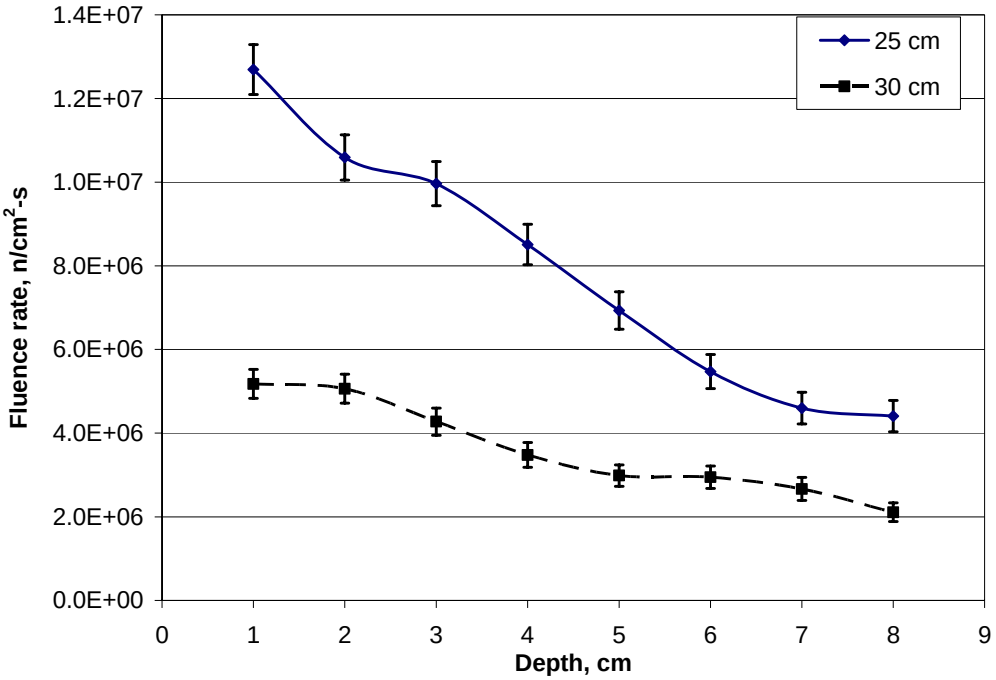

Figure III-11. Neutron fluence rates for two light water moderator thicknesses.

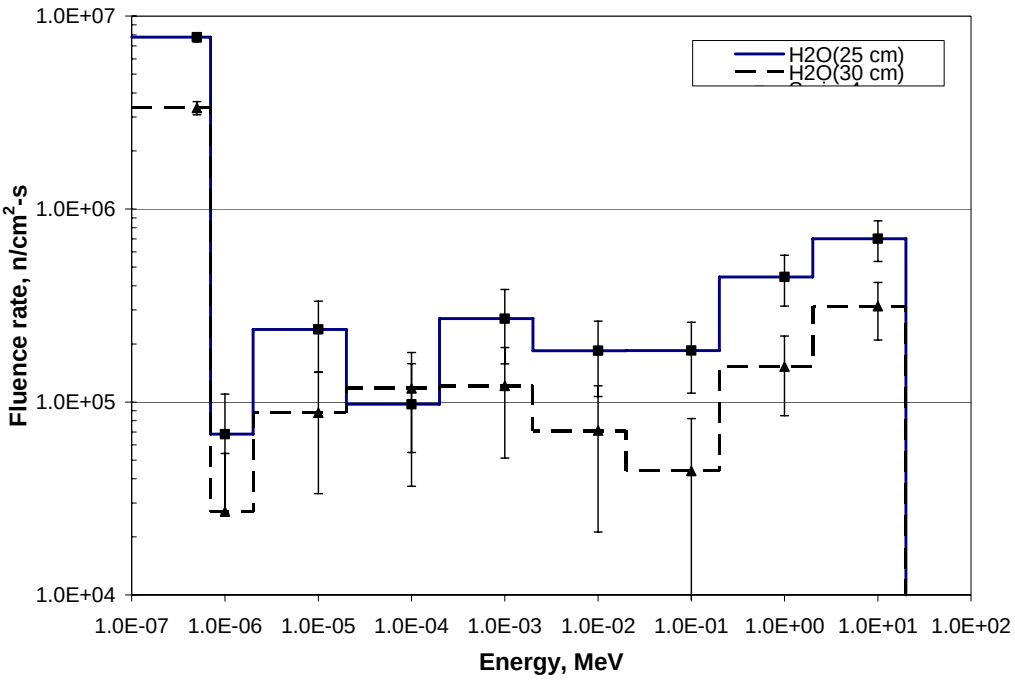

Figure III-12. Neutron spectra for two light water moderator thicknesses at a depth of 3 cm inside a brain phantom.

Table III-3. Different dose components for a 25 cm light water moderator.

Dose components, cGy/min	Depth, cm							
	1	2	3	4	5	6	7	8
$D(RBE)_{fast}$	2.128	2.296	2.232	1.325	1.214	1.082	0.649	0.793
Error	0.428	0.431	0.419	0.299	0.298	0.285	0.209	0.226
$D(RBE)_{photon}$	1.256	1.051	0.942	0.864	0.775	0.706	0.629	0.545
Error	0.047	0.043	0.040	0.039	0.036	0.035	0.032	0.029
$D(RBE)_{14N}$	0.034	0.028	0.026	0.024	0.019	0.014	0.012	0.012
Error	0.005	0.005	0.005	0.004	0.004	0.004	0.003	0.003
$D(RBE)_{10B}$ in tumor	0.815	0.672	0.610	0.557	0.443	0.335	0.293	0.273
Error	0.149	0.136	0.127	0.124	0.114	0.099	0.098	0.094
$D(RBE)_{10B}$ in healthy tissue	0.079	0.066	0.059	0.054	0.043	0.033	0.029	0.027
Error	0.005	0.005	0.004	0.004	0.004	0.003	0.003	0.003
D(RBE) in healthy tissue	3.498	3.441	3.260	2.267	2.051	1.835	1.319	1.376
Error	0.430	0.433	0.421	0.301	0.300	0.287	0.211	0.228
D(RBE) in tumor	4.234	4.047	3.810	2.770	2.451	2.138	1.583	1.622
Error	0.455	0.454	0.440	0.326	0.321	0.304	0.233	0.246
Therapeutic Ratio	1.21	1.18	1.17	1.22	1.20	1.16	1.20	1.18

Table III-4. Different dose components for a 30 cm light water moderator.

Dose components, cGy/min	Depth, cm							
	1	2	3	4	5	6	7	8
$D(RBE)_{fast}$	0.946	0.987	0.944	0.676	0.410	0.453	0.732	0.324
Error	0.247	0.231	0.246	0.195	0.162	0.186	0.233	0.153
$D(RBE)_{photon}$	0.763	0.657	0.607	0.574	0.547	0.462	0.441	0.387
Error	0.033	0.030	0.029	0.029	0.029	0.024	0.026	0.023
$D(RBE)_{14N}$	0.014	0.013	0.011	0.009	0.008	0.008	0.007	0.006
Error	0.003	0.003	0.003	0.003	0.002	0.002	0.002	0.002
$D(RBE)_{10B}$ in tumor	0.327	0.312	0.262	0.216	0.196	0.192	0.162	0.139
Error	0.087	0.087	0.077	0.073	0.065	0.070	0.070	0.060
$D(RBE)_{10B}$ in healthy tissue	0.032	0.030	0.026	0.021	0.019	0.019	0.016	0.014
Error	0.003	0.003	0.003	0.002	0.002	0.002	0.002	0.002
D(RBE) in healthy tissue	1.754	1.688	1.588	1.280	0.984	0.942	1.196	0.731
Error	0.250	0.233	0.248	0.197	0.165	0.187	0.235	0.155
D(RBE) in tumor	2.050	1.970	1.824	1.475	1.161	1.115	1.342	0.856
Error	0.264	0.248	0.260	0.210	0.177	0.200	0.245	0.166
Therapeutic Ratio	1.17	1.17	1.15	1.15	1.18	1.18	1.12	1.17

III – 4 – 2. Results for a carbon moderator

Two different thicknesses of a carbon moderator were considered. The moderator thickness should be larger compared to a light water moderator. Thus, the first calculation was done for a moderator thickness of 30 cm, and the second calculation was done for 40 cm of carbon. The neutron fluence rates for two different carbon moderator thicknesses are shown on Figure III-13. It can be noted, that again, as it was with a light water moderator, the resulting fluence rates are not high enough to provide a reasonable treatment time.

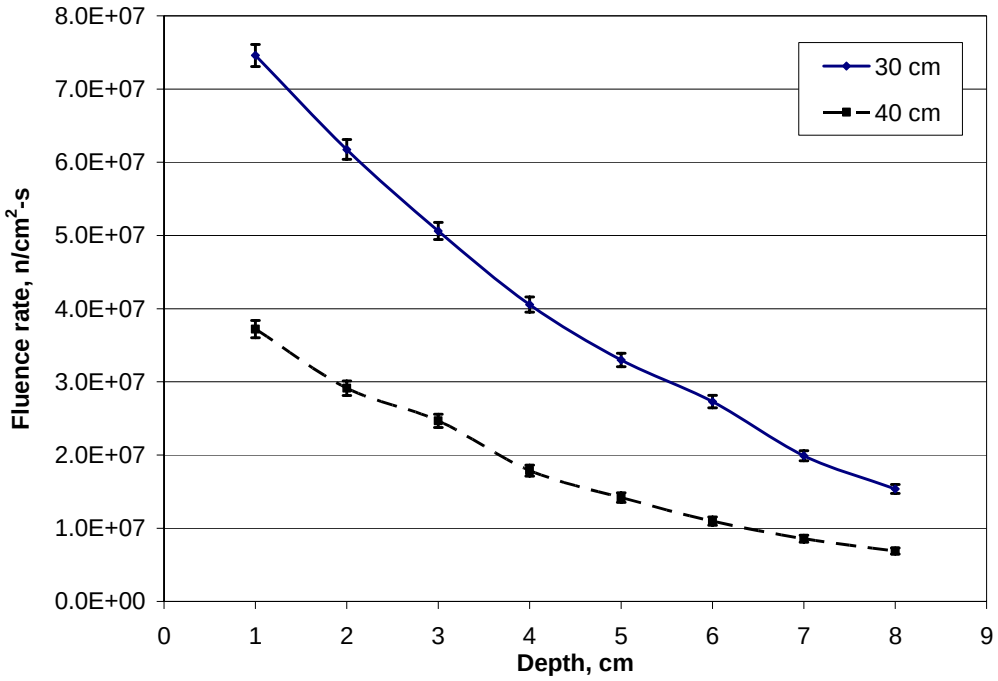

Figure III-13. Neutron fluence rates for two different carbon moderator thicknesses at a depth of 3 cm inside a brain phantom.

A 30-cm thick carbon moderator provides a relatively high fluence rate compared to a light water moderator and it could be considered as a moderation material. The only problem, and it is clearly shown in Figure III-14, is that a 30-cm carbon thickness does not provide a sufficient moderating of neutrons, so the resulting fluence rate has a large fast neutrons component.

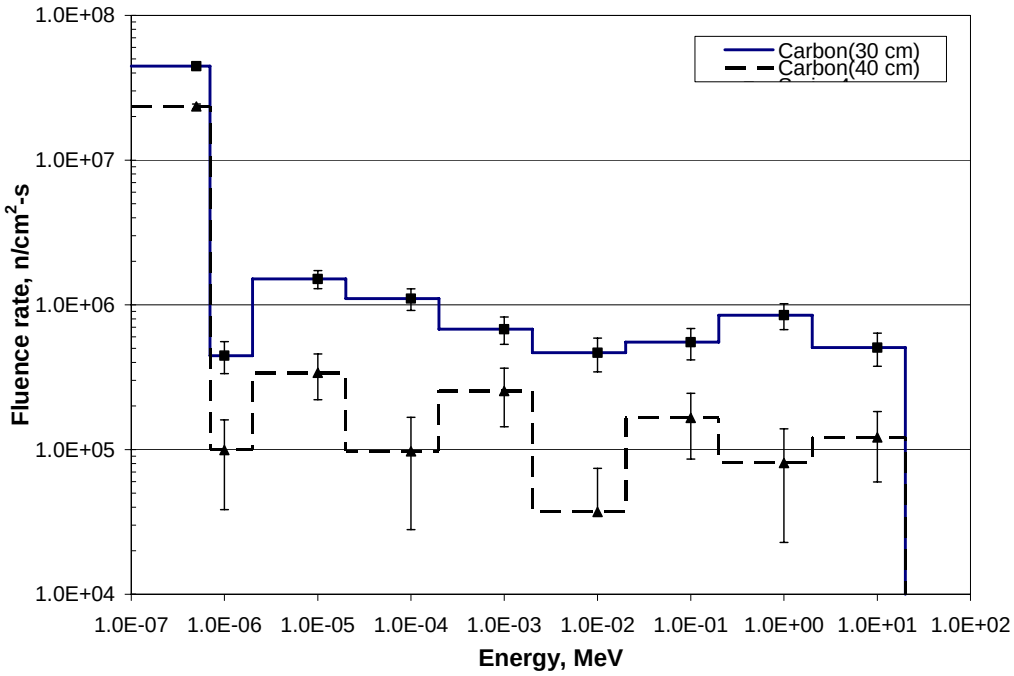

Figure III-14. Neutron spectra for two different carbon moderator thicknesses at a depth of 3 cm inside a brain phantom.

As a result, the therapeutic ratio for a 30 cm carbon moderator is less than 2 and is much lower than that for a 40 cm moderator. The contribution to the total dose in healthy tissue due to fast neutron irradiation ranges from 66 to 75 percent for different depths inside a brain phantom when a 30-cm carbon moderator is used. But using a 40-cm moderator, fast neutrons contribute only from 28 to 59 percent to the total dose in

healthy tissue. Thus, the therapeutic ratio is much higher for a thicker moderator. However, the thicker moderator means a larger distance between the neutron source and the target tumor and, as a result, a low neutron fluence rate. So, it was concluded that a carbon moderator is not suitable for BNCT use, at least for the irradiation geometry considered in this particular research. Different dose components for a carbon moderator of 30 and 40 cm thick are shown in Tables III-5 and III-6.

Table III-5. Different dose components for a 30 cm carbon moderator.

Dose components, cGy/min	Depth, cm							
	1	2	3	4	5	6	7	8
$D(RBE)_{fast}$	3.760	2.537	2.584	2.024	1.776	1.706	1.134	0.889
Error	0.394	0.324	0.359	0.320	0.319	0.303	0.272	0.218
$D(RBE)_{photon}$	0.616	0.523	0.558	0.522	0.460	0.403	0.318	0.302
Error	0.037	0.032	0.033	0.031	0.030	0.029	0.024	0.024
$D(RBE)_{14N}$	0.201	0.174	0.148	0.122	0.099	0.082	0.061	0.046
Error	0.014	0.013	0.012	0.010	0.009	0.008	0.007	0.006
$D(RBE)_{10B}$ in tumor	4.757	4.126	3.491	2.894	2.343	1.933	1.443	1.093
Error	0.398	0.364	0.324	0.293	0.256	0.237	0.196	0.169
$D(RBE)_{10B}$ in healthy tissue	0.464	0.402	0.340	0.282	0.228	0.189	0.141	0.107
Error	0.013	0.012	0.011	0.010	0.009	0.008	0.007	0.006
D(RBE) in healthy tissue	5.041	3.636	3.630	2.951	2.564	2.379	1.653	1.344
Error	0.396	0.326	0.360	0.322	0.321	0.305	0.274	0.219
D(RBE) in tumor	9.334	7.359	6.780	5.563	4.679	4.124	2.955	2.331
Error	0.561	0.488	0.484	0.435	0.410	0.386	0.337	0.277
Therapeutic Ratio	1.85	2.02	1.87	1.89	1.82	1.73	1.79	1.73

Table III-6. Different dose components for a 40 cm carbon moderator.

Dose components, cGy/min	Depth, cm							
	1	2	3	4	5	6	7	8
$D(RBE)_{fast}$	0.995	1.128	0.564	0.328	0.246	0.230	0.133	0.104
Error	0.237	0.267	0.171	0.111	0.110	0.095	0.088	0.066
$D(RBE)_{photon}$	0.320	0.331	0.293	0.294	0.261	0.222	0.215	0.195
Error	0.030	0.029	0.028	0.028	0.029	0.025	0.026	0.023
$D(RBE)_{14N}$	0.112	0.088	0.078	0.057	0.045	0.035	0.028	0.023
Error	0.012	0.010	0.009	0.008	0.007	0.006	0.005	0.004
$D(RBE)_{10B}$ in tumor	2.660	2.089	1.842	1.339	1.064	0.831	0.656	0.533
Error	0.329	0.282	0.262	0.218	0.187	0.165	0.142	0.124
$D(RBE)_{10B}$ in healthy tissue	0.259	0.204	0.180	0.131	0.104	0.081	0.064	0.052
Error	0.011	0.009	0.009	0.007	0.006	0.005	0.005	0.004
D(RBE) in healthy tissue	1.687	1.750	1.114	0.809	0.656	0.569	0.439	0.373
Error	0.240	0.269	0.173	0.115	0.114	0.099	0.092	0.070
D(RBE) in tumor	4.088	3.636	2.777	2.017	1.616	1.319	1.031	0.854
Error	0.407	0.390	0.314	0.247	0.219	0.192	0.169	0.142
Therapeutic Ratio	2.42	2.08	2.49	2.49	2.47	2.32	2.35	2.29

III – 4 – 3. Results for a Fluental™ moderator

Another popular BNCT moderator, called Fluental™, was considered. This moderator has several advantages compared to other moderators which were described in *Chapter III-1-1*. Figure III-15 shows neutron fluence rates for a Fluental™ moderator with thicknesses of 30 and 40 cm.

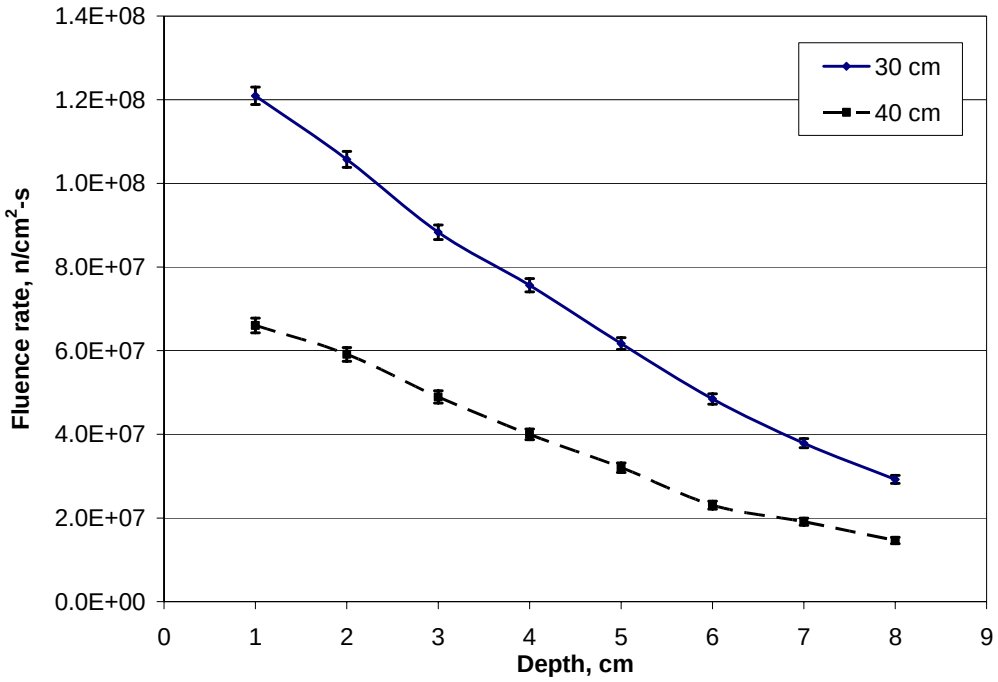

Figure III-15.Neutron fluence rates for two different Fluental™ moderator thicknesses at a depth of 3 cm inside a brain phantom.

The fluence rates obtained were much higher compared to those of carbon. For example, the use of Fluental™ instead of carbon provides a factor of 1.5 – 2 increase in the total fluence rate. But on the other hand, since the Fluental™ moderator consists of elements heavier than carbon, this material has lower moderation ability. Thus, the

neutron spectrum, shown in Figure III-16, has a huge tail because of high energy neutrons which haven't been thermalized enough. This results in a huge contribution to the total dose in healthy tissue due to fast neutrons.

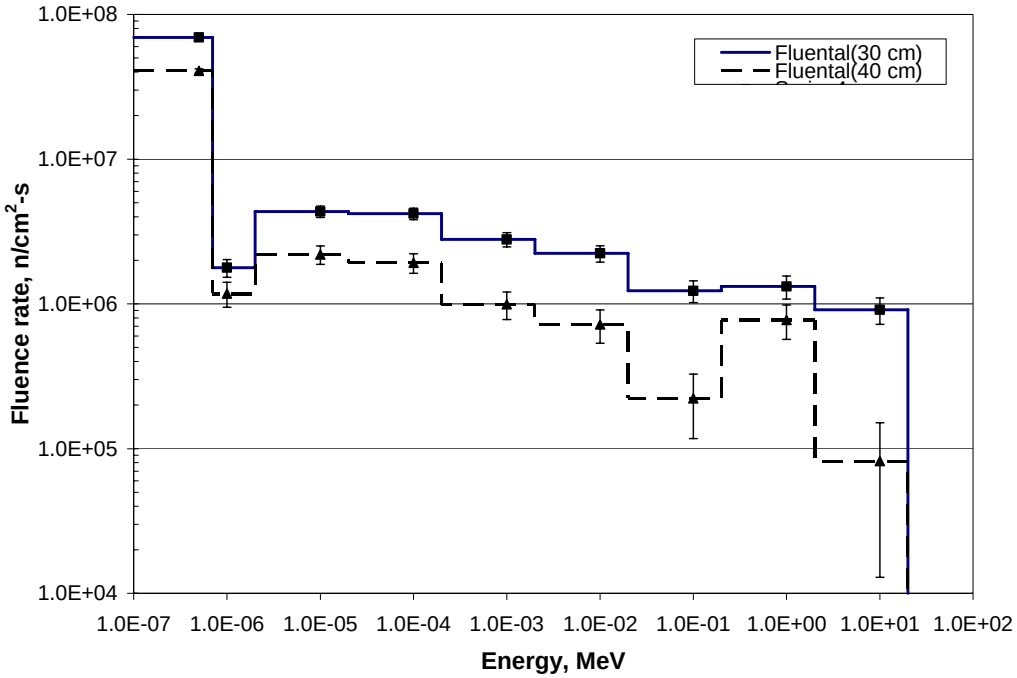

Figure III-16.Neutron spectra for two different Fluental™ moderator thicknesses at a depth of 3 cm inside a brain phantom.

All the dose components along with the therapeutic ratios for different Fluental™ moderator thicknesses are summarized in Table III-7 and III-8. Even though the dose from of fast neutrons contributes up to 87% to the total dose in healthy tissue; the therapeutic ratio is about the same as for a carbon moderator. This is mainly because of a higher thermal fluence rate results in a higher dose to a tumor due to the capture reaction in boron. Thus, it was concluded that Fluental™ is more attractive as a moderating

material than carbon, since it provides the same therapeutic ratios with a higher fluence rate of thermal neutrons, which eventually decreases the treatment time.

Table III-7. Different dose components for a 30 cm Fluental^{TM} moderator.

Dose components, cGy/min	Depth, cm							
	1	2	3	4	5	6	7	8
$D(RBE)_{fast}$	10.65	6.91	5.01	4.44	2.54	2.10	1.62	1.66
Error	0.784	0.616	0.531	0.505	0.375	0.332	0.305	0.318
$D(RBE)_{photon}$	0.786	0.775	0.825	0.798	0.819	0.645	0.549	0.511
Error	0.043	0.044	0.044	0.044	0.044	0.039	0.036	0.036
$D(RBE)_{14N}$	0.254	0.255	0.230	0.209	0.180	0.144	0.114	0.089
Error	0.017	0.017	0.016	0.015	0.014	0.012	0.011	0.009
$D(RBE)_{10B}$ in tumor	6.01	6.02	5.45	4.94	4.25	3.40	2.71	2.10
Error	0.479	0.474	0.445	0.426	0.384	0.341	0.300	0.266
$D(RBE)_{10B}$ in healthy tissue	0.586	0.587	0.531	0.482	0.414	0.332	0.264	0.205
Error	0.016	0.016	0.015	0.014	0.013	0.011	0.010	0.009
D(RBE) in healthy tissue	12.28	8.52	6.59	5.93	3.95	3.22	2.55	2.47
Error	0.786	0.618	0.533	0.508	0.378	0.335	0.307	0.320
D(RBE) in tumor	17.70	13.96	11.51	10.39	7.78	6.29	4.99	4.36
Error	0.920	0.778	0.695	0.663	0.539	0.478	0.429	0.416
Therapeutic Ratio	1.44	1.64	1.75	1.75	1.97	1.95	1.96	1.77

Table III-8. Different dose components for a 40 cm Fluental™ moderator.

Dose components, cGy/min	Depth, cm							
	1	2	3	4	5	6	7	8
$D(RBE)_{fast}$	3.53	1.85	1.69	1.25	0.47	0.32	0.34	0.11
Error	0.46	0.25	0.29	0.28	0.13	0.12	0.13	0.07
$D(RBE)_{photon}$	0.477	0.514	0.468	0.486	0.398	0.381	0.320	0.242
Error	0.039	0.041	0.039	0.039	0.035	0.036	0.031	0.027
$D(RBE)_{14N}$	0.150	0.151	0.135	0.117	0.097	0.072	0.060	0.047
Error	0.015	0.015	0.014	0.013	0.011	0.009	0.009	0.008
$D(RBE)_{10B}$ in tumor	3.55	3.57	3.20	2.77	2.29	1.69	1.43	1.11
Error	0.41	0.41	0.40	0.36	0.32	0.27	0.25	0.22
$D(RBE)_{10B}$ in healthy tissue	0.347	0.348	0.312	0.270	0.224	0.165	0.139	0.109
Error	0.01	0.014	0.013	0.012	0.011	0.009	0.008	0.007
D(RBE) in healthy tissue	4.51	2.86	2.60	2.12	1.19	0.93	0.86	0.50
Error	0.464	0.251	0.295	0.287	0.138	0.123	0.138	0.073
D(RBE) in tumor	7.71	6.08	5.49	4.62	3.26	2.46	2.15	1.51
Error	0.621	0.482	0.496	0.457	0.351	0.293	0.283	0.231
Therapeutic Ratio	1.71	2.13	2.11	2.18	2.74	2.64	2.49	3.00

III – 4 – 4. Results for a heavy water moderator

The most promising results were obtained with a heavy water moderator. Four different thicknesses were investigated – 25, 30, 40 and 50 cm. Neutron fluence rates were higher or at least of the same order of magnitude compared to other types of moderating materials used in this research, see Figure III-17.

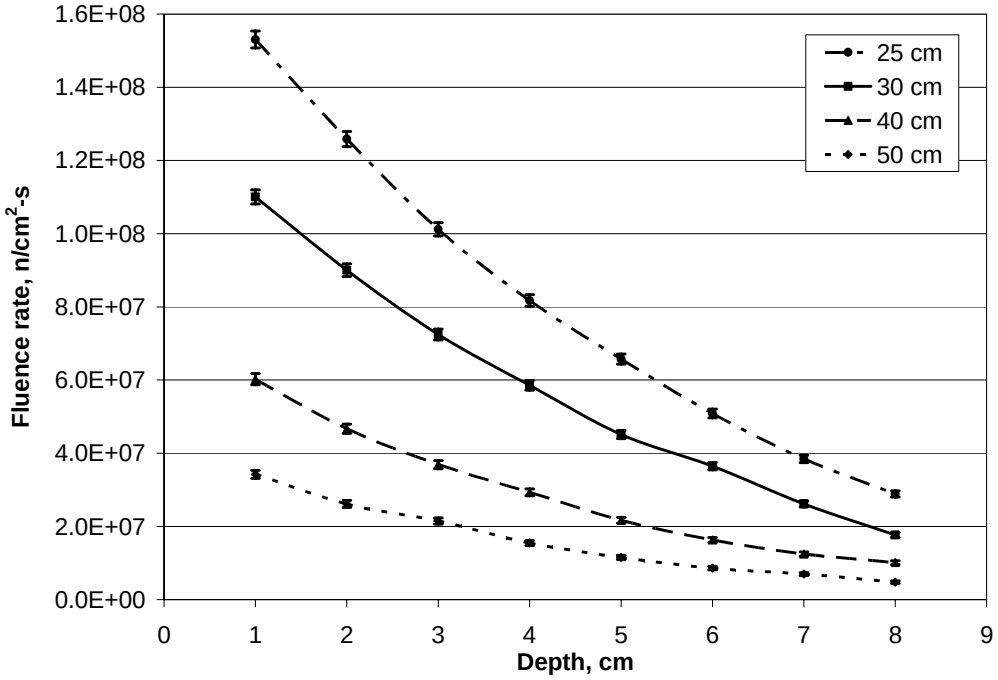

Figure III-17. Neutron fluence rates for two different heavy water moderator thicknesses at a depth of 3 cm inside a brain phantom.

Since heavy water is a good moderator, neutrons could significantly slow down even in a 25 cm layer of this material. So, the fast component of a neutron fluence rate was not high. Moreover, after moderating with heavy water having thickness of 40 cm or more the neutron fluence rate inside a brain phantom was comprised almost totally of

thermal neutrons. The neutron spectra for thicknesses of 25 cm and 30 cm are shown in Figure III-18.

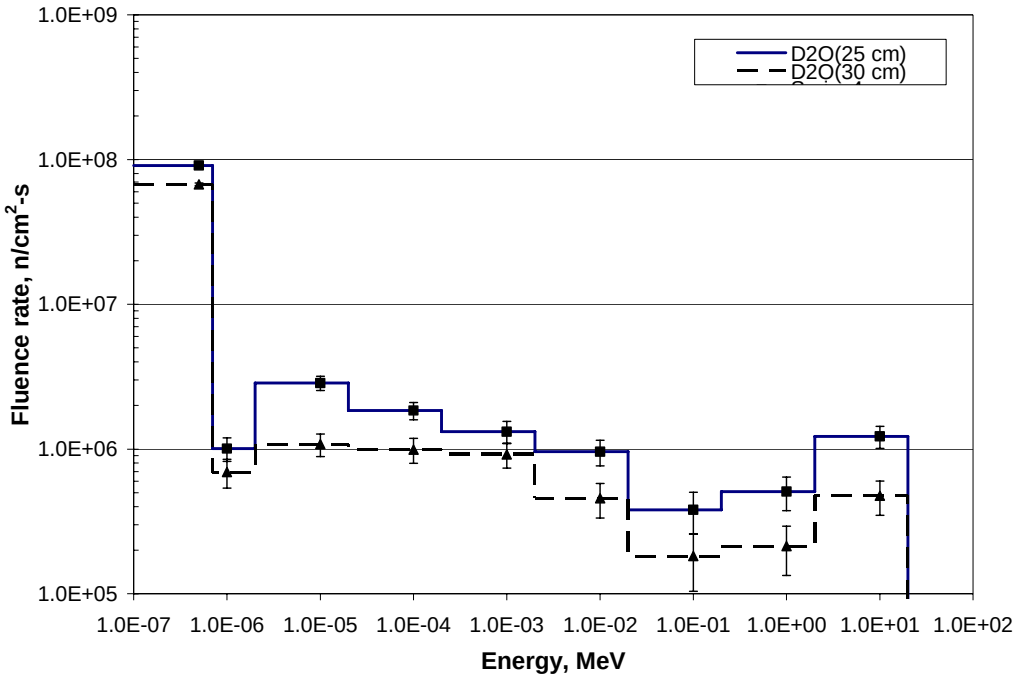

Figure III-18. Neutron spectra for two different heavy water moderator thicknesses at a depth of 3 cm inside a brain phantom.

Tables III-9, III-10, III-11 and III-12 show contributions of each dose component to the total dose for all four thicknesses of heavy water. Good neutron thermalization resulted in therapeutic ratios of 2 or more depending on how much moderator material was placed between a neutron source and the particular target at a certain depth inside a brain phantom. Three out of the four thicknesses were rejected for future analysis. The neutron spectrum from a 25 cm thick moderator still suffered from high energy neutrons that reduced the therapeutic ratio. Moderator thicknesses of 40 and 50 cm showed good

treatment abilities compared to other moderators but the neutron fluence rate was too low to provide treatment in a reasonable time. Thus, a heavy water moderator, having thickness of 30 cm, was chosen for future investigation and comparison.

Table III-9. Different dose components for a 25 cm heavy water moderator.

Dose components, cGy/min	Depth, cm							
	1	2	3	4	5	6	7	8
$D(RBE)_{fast}$	6.84	4.25	4.47	3.51	2.73	1.84	1.60	1.00
Error	0.60	0.44	0.54	0.49	0.43	0.32	0.32	0.25
$D(RBE)_{photon}$	1.458	1.427	1.153	1.119	1.060	0.902	0.808	0.685
Error	0.056	0.056	0.047	0.048	0.046	0.042	0.040	0.038
$D(RBE)_{14N}$	0.42	0.37	0.30	0.25	0.20	0.16	0.12	0.09
Error	0.022	0.020	0.018	0.016	0.014	0.012	0.010	0.009
$D(RBE)_{10B}$ in tumor	9.83	8.65	7.14	5.82	4.82	3.71	2.83	2.15
Error	0.62	0.57	0.50	0.44	0.39	0.34	0.29	0.25
$D(RBE)_{10B}$ in healthy tissue	0.96	0.844	0.697	0.568	0.470	0.362	0.276	0.209
Error	0.02	0.019	0.017	0.015	0.013	0.011	0.010	0.008
D(RBE) in healthy tissue	9.67	6.89	6.62	5.45	4.46	3.26	2.80	1.98
Error	0.599	0.449	0.544	0.488	0.435	0.325	0.327	0.254
D(RBE) in tumor	18.54	14.70	13.07	10.70	8.81	6.61	5.36	3.92
Error	0.859	0.725	0.740	0.657	0.587	0.469	0.438	0.356
Therapeutic Ratio	1.92	2.13	1.97	1.96	1.98	2.03	1.91	1.98

Table III-10. Different dose components for a 30 cm heavy water moderator.

Dose components, cGy/min	Depth, cm							
	1	2	3	4	5	6	7	8
$D(RBE)_{fast}$	2.74	2.38	1.63	1.34	1.47	1.47	1.40	0.40
Error	0.43	0.40	0.32	0.33	0.32	0.36	0.32	0.17
$D(RBE)_{photon}$	1.021	1.054	0.906	0.866	0.794	0.731	0.622	0.538
Error	0.047	0.048	0.044	0.043	0.042	0.042	0.037	0.035
$D(RBE)_{14N}$	0.327	0.273	0.224	0.183	0.142	0.115	0.082	0.057
Error	0.019	0.017	0.015	0.014	0.012	0.010	0.009	0.007
$D(RBE)_{10B}$ in tumor	7.74	6.45	5.29	4.32	3.36	2.73	1.95	1.34
Error	0.55	0.49	0.43	0.38	0.33	0.28	0.24	0.19
$D(RBE)_{10B}$ in healthy tissue	0.755	0.629	0.516	0.421	0.327	0.266	0.190	0.131
Error	0.02	0.016	0.014	0.013	0.011	0.009	0.008	0.006
D(RBE) in healthy tissue	4.84	4.34	3.28	2.81	2.73	2.58	2.29	1.13
Error	0.435	0.401	0.327	0.335	0.327	0.361	0.321	0.173
D(RBE) in tumor	11.83	10.16	8.05	6.71	5.76	5.05	4.05	2.34
Error	0.699	0.633	0.537	0.508	0.461	0.459	0.403	0.259
Therapeutic Ratio	2.44	2.34	2.46	2.39	2.11	1.95	1.77	2.07

Table III-11. Different dose components for a 40 cm heavy water moderator.

Dose components, cGy/min	Depth, cm							
	1	2	3	4	5	6	7	8
$D(RBE)_{fast}$	1.069	0.936	0.274	0.251	0.283	0.597	0.390	0.092
Error	0.256	0.254	0.100	0.099	0.123	0.239	0.172	0.058
$D(RBE)_{photon}$	0.632	0.578	0.585	0.547	0.482	0.414	0.364	0.307
Error	0.041	0.039	0.040	0.038	0.037	0.034	0.031	0.027
$D(RBE)_{14N}$	0.190	0.148	0.119	0.096	0.071	0.052	0.040	0.033
Error	0.016	0.013	0.012	0.010	0.008	0.007	0.006	0.005
$D(RBE)_{10B}$ in tumor	4.489	3.499	2.814	2.264	1.681	1.241	0.947	0.788
Error	0.442	0.367	0.324	0.284	0.235	0.196	0.164	0.153
$D(RBE)_{10B}$ in healthy tissue	0.438	0.341	0.274	0.221	0.164	0.121	0.092	0.077
Error	0.015	0.012	0.011	0.009	0.008	0.007	0.005	0.005
D(RBE) in healthy tissue	2.329	2.003	1.252	1.115	1.000	1.185	0.887	0.510
Error	0.260	0.258	0.109	0.107	0.129	0.241	0.175	0.064
D(RBE) in tumor	6.380	5.161	3.792	3.158	2.518	2.305	1.741	1.220
Error	0.512	0.448	0.342	0.303	0.268	0.311	0.240	0.166
Therapeutic Ratio	2.74	2.58	3.03	2.83	2.52	1.95	1.96	2.39

Table III-12. Different dose components for a 50 cm heavy water moderator.

Dose components, cGy/min	Depth, cm							
	1	2	3	4	5	6	7	8
$D(RBE)_{fast}$	0.377	0.146	0.132	0.082	0.109	0.046	0.103	0.033
Error	0.152	0.087	0.076	0.063	0.070	0.044	0.072	0.031
$D(RBE)_{photon}$	0.444	0.388	0.352	0.312	0.325	0.276	0.225	0.261
Error	0.038	0.032	0.033	0.031	0.031	0.029	0.025	0.029
$D(RBE)_{14N}$	0.112	0.086	0.071	0.051	0.038	0.029	0.023	0.015
Error	0.012	0.010	0.009	0.007	0.006	0.005	0.004	0.004
$D(RBE)_{10B}$ in tumor	2.647	2.040	1.672	1.209	0.899	0.676	0.542	0.366
Error	0.329	0.288	0.249	0.207	0.172	0.145	0.126	0.101
$D(RBE)_{10B}$ in healthy tissue	0.258	0.199	0.163	0.118	0.088	0.066	0.053	0.036
Error	0.011	0.010	0.008	0.007	0.006	0.005	0.004	0.003
D(RBE) in healthy tissue	1.190	0.819	0.718	0.563	0.559	0.417	0.404	0.346
Error	0.157	0.094	0.084	0.070	0.077	0.053	0.077	0.043
D(RBE) in tumor	3.579	2.660	2.227	1.654	1.371	1.027	0.893	0.676
Error	0.364	0.302	0.263	0.218	0.188	0.155	0.148	0.109
Therapeutic Ratio	3.01	3.25	3.10	2.94	2.45	2.47	2.21	1.96

III – 4 – 5. Filtering experiment

Two different moderators were selected for a filtering experiment based on the results presented above – heavy water and Fluental™, both having thickness of 30 cm. The heavy water moderator showed relatively high therapeutic ratio with decent dose rates inside a brain phantom. The Fluental™ moderator didn't provide a high therapeutic ratio, but dose rates were significantly higher than those for a heavy water moderator of the same thickness.

The geometry used for a filtering experiment is shown in Figure III-19.

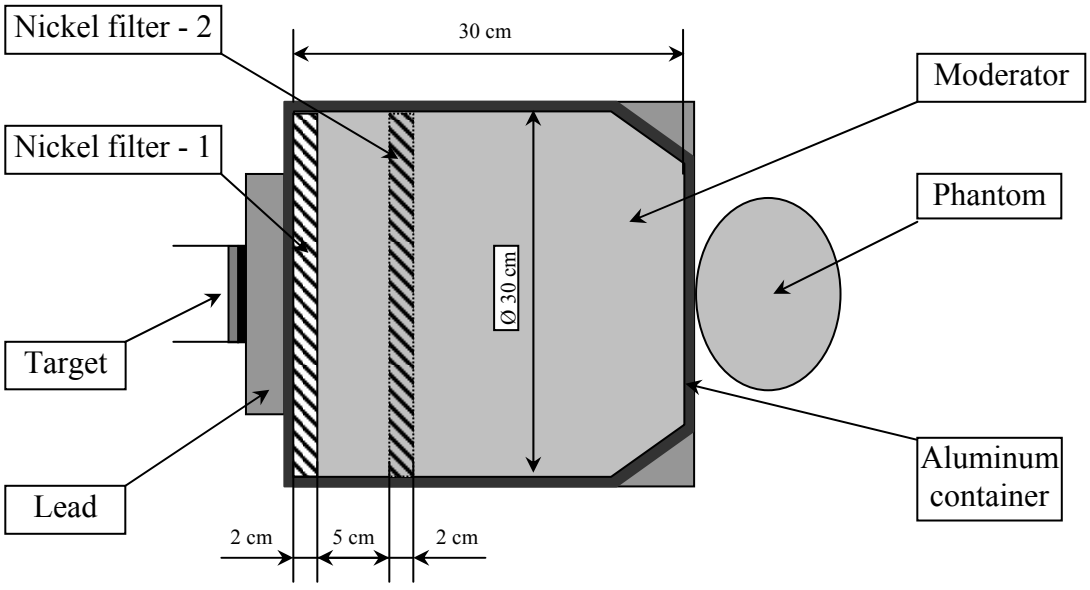

Figure III-19. Geometry used for a filtering experiment.

Considering the information presented in Chapter III – 1 – 2, a nickel filter was investigated to improve spectral characteristics of moderating neutrons. Neutron energies were expected to shift to the epithermal region thus reducing the dose to scalp

and skull from thermal neutrons and increasing the therapeutic ratio for brain tissue. The total cross-section of nickel is on the order of few tens of barns. This suggests a neutron mean free path in nickel equal to 1 – 2 millimeters. Thus, the thickness of a nickel filter was set to at least ten neutron mean free paths or about to 2 cm. Two different filter positions were considered in order to investigate any differences in the resulting neutron spectrum. The "left" position (Nickel filter – 1 on Figure III-19) when the filter was placed next to the neutron source and the "intermediate" position (Nickel filter – 2 on Figure III-19), when the filter was placed inside the moderator medium at a 7-cm depth. The total neutron fluence rates for both positions are shown in Figures III-20 and III-21. The filtered fluence rates came out to be lower by 20 – 30 percent compared to those obtained without filtering. This is because of the significantly higher nickel absorption cross-section compared to that of heavy water or Fluental^{TM}, see Figures III-3 and III-5 above. Moreover, the total fluence rate obtained with a filter in the "intermediate" position is lower than the fluence rate when a filter in the "left" position was used. This was due to the moderation of incident neutrons. Neutrons hitting a filter in the "intermediate" position had lower average energies because of slowing down in 7 cm of moderation material. The lower neutron energy means the higher nickel absorption cross-section and, thus, the resulting lower fluence rate.

The calculated results for different dose components for both moderators and two different geometries are given in Tables III-13-16. A nickel filter, when used, replaced a part of a moderating material. This influences the fluence rate in two competing ways – reducing a total fluence rate due to absorption, as it is described above, but also

increasing the fast part of a fluence rate due to the smaller moderator thickness. Note that the total doses to a tumor and healthy tissue are reduced for both moderators because of the lower fluence rate of thermal neutrons.

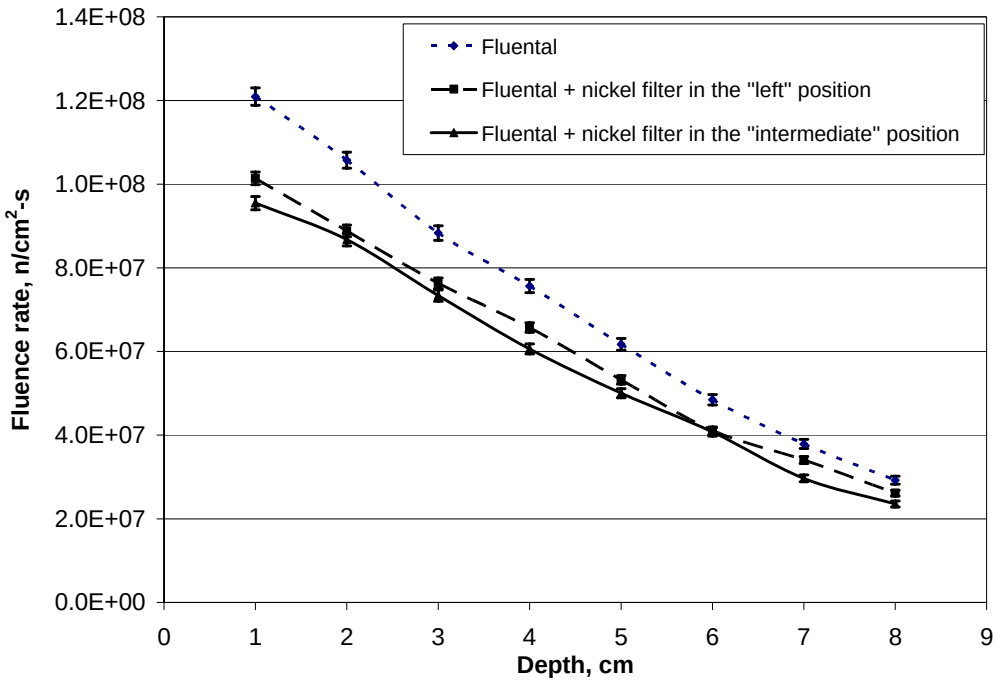

Figure III-20. The neutron fluence rate for a Fluental^{TM} moderator with and without a nickel filter.

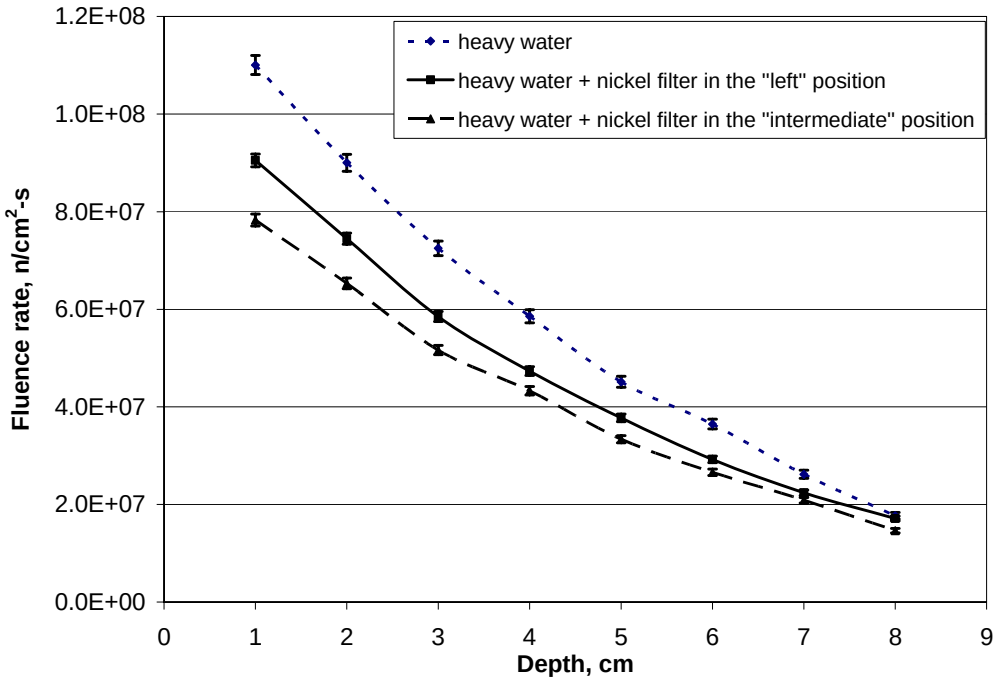

Figure III-21. The neutron fluence rate for a heavy water moderator with and without a nickel filter.

The dose from fast neutrons is also reduced for a Fluental^{TM} moderator, but for heavy water it increased. This is because heavy water is a much better moderator than the Fluental^{TM}, so decreasing of moderator thickness significantly increases the fast fluence rate component.

Another calculation was made to see a difference between natural nickel filter and a ^{60}Ni filter. Ni-60 has several benefits compared to natural nickel and that was discussed in *Chapter III-1-2*. One of them is a lower neutron absorption cross-section for the whole energy range compared to natural nickel. This leads to a higher resulting neutron fluence rate and a lower photon dose, see Figure III-22 and Table III-17. Also, ^{60}Ni has a much lower scattering cross-section compared to natural nickel for low-

energy neutrons. This means the dose to tissue due to fast neutrons will be higher if the ^{60}Ni filter is used instead of natural nickel, see Table III-17. For these reasons, ^{60}Ni yields a higher therapeutic ratio compared to a natural nickel filter in the same geometry. However, the fluence rate is still much less than that for the geometry with no filter.

Thus, the use of a nickel filter didn't show any benefits in term of therapeutic ratios, and, since the total fluence rate was also reduced, the moderator assemblies containing no filter were chosen for a final comparison.

Table III-13. Different dose components for a 28 cm heavy water moderator and 2 cm nickel filter in the "left" position.

Dose components, cGy/min	Depth, cm							
	1	2	3	4	5	6	7	8
$D(RBE)_{fast}$	3.315	2.873	1.816	1.571	1.299	0.920	0.939	1.052
Error	0.307	0.311	0.240	0.226	0.215	0.183	0.175	0.207
$D(RBE)_{photon}$	1.332	1.314	1.161	1.108	0.975	0.916	0.826	0.760
Error	0.041	0.040	0.038	0.037	0.035	0.034	0.032	0.031
$D(RBE)_{14N}$	0.257	0.218	0.178	0.146	0.119	0.092	0.071	0.054
Error	0.013	0.012	0.010	0.009	0.008	0.007	0.006	0.005
$D(RBE)_{10B}$ in tumor	6.076	5.165	4.204	3.450	2.806	2.184	1.679	1.270
Error	0.363	0.324	0.288	0.253	0.225	0.191	0.165	0.140
$D(RBE)_{10B}$ in healthy tissue	0.592	0.504	0.410	0.336	0.274	0.213	0.164	0.124
Error	0.012	0.011	0.010	0.008	0.008	0.006	0.005	0.005
D(RBE) in healthy tissue	5.496	4.910	3.564	3.160	2.666	2.140	1.999	1.990
Error	0.310	0.314	0.244	0.229	0.218	0.186	0.178	0.209
D(RBE) in tumor	10.98	9.57	7.36	6.27	5.20	4.11	3.51	3.14
Error	0.48	0.45	0.38	0.34	0.31	0.27	0.24	0.25
Therapeutic Ratio	2.00	1.95	2.06	1.99	1.95	1.92	1.76	1.58

Table III-14. Different dose components for a 28 cm heavy water moderator and 2 cm nickel filter in the "intermediate" position.

Dose components, cGy/min	Depth, cm							
	1	2	3	4	5	6	7	8
$D(RBE)_{fast}$	3.334	2.310	1.550	1.712	1.477	1.030	0.978	0.721
Error	0.326	0.255	0.216	0.251	0.237	0.196	0.196	0.150
$D(RBE)_{photon}$	1.332	1.347	1.179	1.126	1.005	0.905	0.779	0.709
Error	0.041	0.042	0.040	0.038	0.036	0.035	0.031	0.030
$D(RBE)_{14N}$	0.217	0.191	0.157	0.132	0.103	0.083	0.066	0.046
Error	0.012	0.011	0.009	0.009	0.007	0.007	0.006	0.005
$D(RBE)_{10B}$ in tumor	5.141	4.519	3.703	3.129	2.445	1.966	1.563	1.080
Error	0.330	0.304	0.266	0.241	0.208	0.187	0.162	0.130
$D(RBE)_{10B}$ in healthy tissue	0.501	0.441	0.361	0.305	0.238	0.192	0.152	0.105
Error	0.011	0.010	0.009	0.008	0.007	0.006	0.005	0.004
D(RBE) in healthy tissue	5.385	4.289	3.246	3.276	2.824	2.210	1.976	1.581
Error	0.329	0.259	0.220	0.254	0.240	0.199	0.199	0.153
D(RBE) in tumor	10.03	8.37	6.59	6.10	5.03	3.98	3.39	2.56
Error	0.47	0.40	0.35	0.35	0.32	0.27	0.26	0.20
Therapeutic Ratio	1.86	1.95	2.03	1.86	1.78	1.80	1.71	1.62

Table III-15. Different dose components for a 28 cm Fluental™ moderator and 2 cm nickel filter in the "left" position.

Dose components, cGy/min	Depth, cm							
	1	2	3	4	5	6	7	8
$D(RBE)_{fast}$	8.003	6.130	4.542	3.522	2.612	1.886	1.814	1.508
Error	0.470	0.441	0.392	0.340	0.299	0.256	0.270	0.251
$D(RBE)_{photon}$	0.787	0.719	0.687	0.745	0.613	0.560	0.499	0.416
Error	0.035	0.033	0.032	0.033	0.030	0.029	0.027	0.024
$D(RBE)_{14N}$	0.203	0.208	0.194	0.178	0.153	0.121	0.102	0.078
Error	0.012	0.012	0.011	0.011	0.010	0.009	0.008	0.007
$D(RBE)_{10B}$ in tumor	4.791	4.912	4.593	4.214	3.625	2.853	2.419	1.852
Error	0.335	0.336	0.319	0.306	0.281	0.244	0.227	0.191
$D(RBE)_{10B}$ in healthy tissue	0.467	0.479	0.448	0.411	0.353	0.278	0.236	0.181
Error	0.011	0.011	0.011	0.010	0.009	0.008	0.008	0.006
D(RBE) in healthy tissue	9.460	7.536	5.870	4.856	3.732	2.844	2.650	2.183
Error	0.472	0.442	0.394	0.342	0.301	0.258	0.272	0.252
D(RBE) in tumor	13.78	11.97	10.02	8.66	7.00	5.42	4.83	3.85
Error	0.58	0.56	0.51	0.46	0.41	0.36	0.35	0.32
Therapeutic Ratio	1.46	1.59	1.71	1.78	1.88	1.91	1.82	1.77

Table III-16. Different dose components for a 28 cm Fluental^{TM} moderator and 2 cm nickel filter in the "intermediate" position.

Dose components, cGy/min	Depth, cm							
	1	2	3	4	5	6	7	8
$D(RBE)_{fast}$	8.189	6.075	4.117	3.093	1.978	2.205	1.701	1.239
Error	0.534	0.478	0.394	0.362	0.281	0.330	0.266	0.232
$D(RBE)_{photon}$	0.715	0.726	0.757	0.731	0.688	0.558	0.532	0.453
Error	0.035	0.036	0.036	0.037	0.036	0.031	0.031	0.028
$D(RBE)_{14N}$	0.190	0.202	0.189	0.168	0.143	0.117	0.089	0.071
Error	0.013	0.013	0.012	0.011	0.011	0.009	0.008	0.007
$D(RBE)_{10B}$ in tumor	4.504	4.786	4.470	3.963	3.382	2.771	2.099	1.679
Error	0.356	0.366	0.348	0.321	0.298	0.264	0.225	0.198
$D(RBE)_{10B}$ in healthy tissue	0.439	0.467	0.436	0.386	0.330	0.270	0.205	0.164
Error	0.012	0.012	0.012	0.011	0.010	0.009	0.008	0.007
D(RBE) in healthy tissue	9.534	7.470	5.498	4.378	3.138	3.150	2.526	1.926
Error	0.535	0.479	0.396	0.364	0.284	0.332	0.268	0.234
D(RBE) in tumor	13.60	11.79	9.53	7.95	6.19	5.65	4.42	3.44
Error	0.64	0.60	0.53	0.49	0.41	0.42	0.35	0.31
Therapeutic Ratio	1.43	1.58	1.73	1.82	1.97	1.79	1.75	1.79

Table III-17. Different dose components for a 28 cm heavy water moderator and 2 cm ^{60}Ni filter in the "left" position.

Dose components, cGy/min	Depth, cm							
	1	2	3	4	5	6	7	8
$D(RBE)_{fast}$	3.282	2.715	2.178	1.885	1.243	1.120	0.786	0.992
Error	0.349	0.352	0.329	0.297	0.260	0.238	0.183	0.243
$D(RBE)_{photon}$	1.053	1.003	0.947	0.826	0.769	0.730	0.623	0.565
Error	0.044	0.043	0.042	0.039	0.039	0.037	0.035	0.033
$D(RBE)_{14N}$	0.278	0.231	0.193	0.156	0.129	0.092	0.074	0.057
Error	0.016	0.014	0.013	0.011	0.010	0.008	0.007	0.006
$D(RBE)_{10B}$ in tumor	6.587	5.470	4.559	3.685	3.058	2.174	1.749	1.342
Error	0.453	0.405	0.357	0.312	0.279	0.228	0.203	0.173
$D(RBE)_{10B}$ in healthy tissue	0.642	0.533	0.444	0.359	0.298	0.212	0.171	0.131
Error	0.015	0.014	0.012	0.010	0.009	0.008	0.007	0.006
D(RBE) in healthy tissue	5.256	4.482	3.763	3.226	2.439	2.154	1.653	1.745
Error	0.353	0.355	0.332	0.300	0.264	0.241	0.187	0.246
D(RBE) in tumor	11.20	9.42	7.88	6.55	5.20	4.12	3.23	2.96
Error	0.57	0.54	0.49	0.43	0.38	0.33	0.28	0.30
Therapeutic Ratio	2.13	2.10	2.09	2.03	2.13	1.91	1.95	1.69

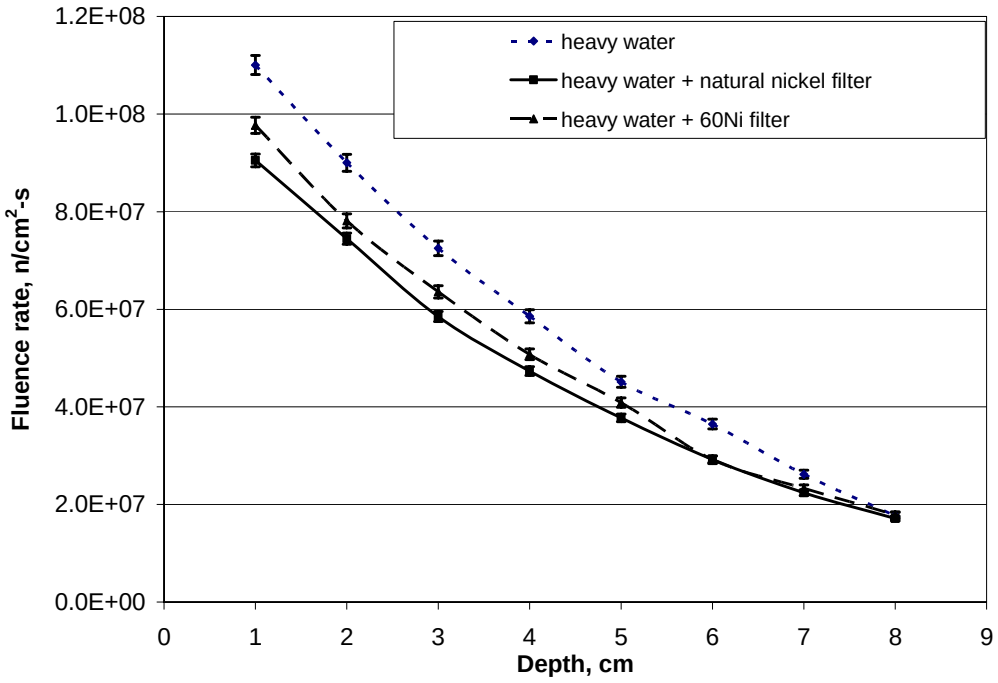

Figure III-22. Comparison of natural nickel and ^{60}Ni filters.

III – 4 – 6. Comparison of the most suitable moderators

The two different geometries that showed the most promise were selected based on the calculated results. The first moderating geometry is 30 cm of heavy water. The second geometry includes a 40 cm thick Fluental™ moderator. These two geometries showed very similar results see Table III-8 and Table III-10 above. Thermal neutrons and photons produced a lower dose to healthy tissue in both cases compared to that from fast neutrons. This is especially appreciable for a Fluental™ moderator and shallow depths inside a brain phantom. The main problem for both geometries is the fast neutron dose. The larger moderator thickness provides less fast neutrons but increases a treatment time. Thus, a compromise must be found between these two quantities.

One of the most significant clinical requirements, namely that the dose to the healthy brain tissue must be kept below its tolerance limit, has to be considered. According to the protocol used at the Brookhaven Medical Research Reactor (BMRR), the maximum dose to the normal brain is set to 12.5 RBEGy (Bleuel *et al* 1998), which for the conditions of these two experiments, supposing a 60 μA beam current, would be reached for a treatment time of 258 min with a heavy water moderator and 277 min with a Fluental™ moderator. The RBE-dose rates obtained from calculations are plotted in Figures III-23 and III-24. For a heavy water moderator the advantage depth is 6.2 cm and, if a Fluental™ moderator is used, this depth is 4 cm. Thus, heavy water looks preferable to a Fluental™ moderator in terms of using it for boron neutron capture therapy. Combinations of Fluental™ and heavy water could be used but only small gains could be realized.

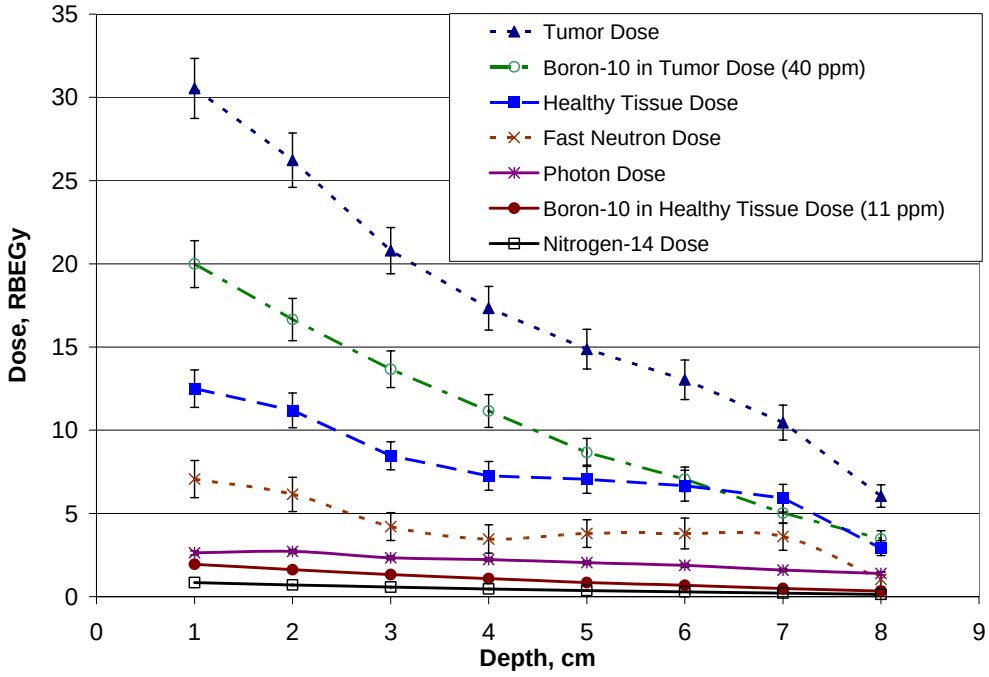

Figure III-23. RBE-dose for a 258 min treatment with a heavy water moderator.

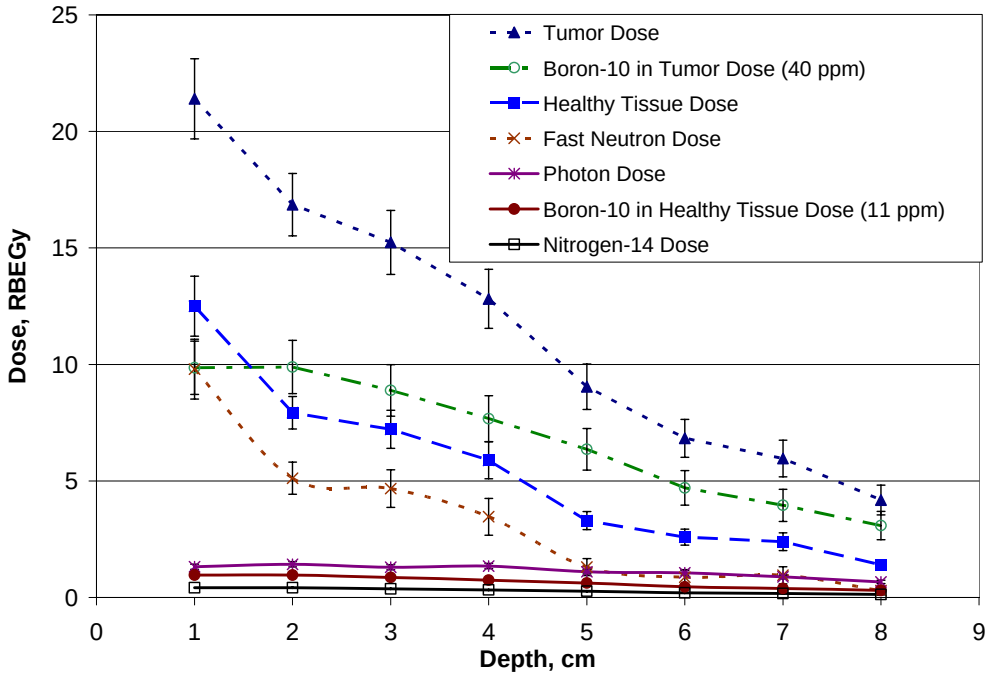

Figure III-24. RBE-dose for a 277 min treatment with a Fluental™ moderator.

CHAPTER IV

CONCLUSIONS AND DISCUSSION

Boron neutron capture therapy (BNCT) is under active investigation all over the world. Historically the best source of neutrons was a nuclear reactor. However, disadvantages of reactor are the high capital costs are very high and reactors are too complicated for an ordinary clinic to operate, so these clinics cannot afford to build and maintain a small nuclear reactor to use as a neutron source.

Another approach to this problem is to use particle accelerators. These machines can accelerate protons or deuterons to the required energies for the reaction and the bombarded target emits neutrons. If the beam current and reaction cross-section is high then the neutrons can be obtained at rates and energy levels appropriate for BNCT. There are a number of advantages of using accelerators as a neutron source for BNCT. They are cheaper, easier to operate, and are pose less overall risk than nuclear reactors. Accelerator neutron sources are well understood and implemented in a number of research facilities (Wang *et al* 1989).

This dissertation has produced a first look at using the particular GE PETtrace cyclotron with ^{18}O target for BNCT. Many facilities, such as nuclear pharmacies and hospitals are using this cyclotron for medical radionuclide production. These cyclotrons are designed mostly for fluorodeoxyglucose (FDG) production. FDG is manufactured in an automated synthesis unit from ^{18}F. This nuclide is produced in a cyclotron by proton bombardment of enriched water (^{18}O). The efficiency of cyclotron use may be

significantly increased if unused neutrons could be utilized for BNCT at the same time as radionuclide production.

While bombarding with protons the ^{18}O target emits neutrons. The resulting dose from the radiation emitted from the target is evaluated using the Monte Carlo radiation transport code MCNP at several depths in a brain phantom for several scattering geometries. Each geometry includes a moderator assembly surrounded by a thick carbon reflector.

The moderator assembly consists of an aluminum container filled with a moderating material. Several different types of materials were investigated to moderate neutrons to the epithermal energies: light water, carbon, heavy water and Fluental^{TM} that consists of aluminum, fluorine and natural lithium (Auterinen *et al* 1993). Various thicknesses of moderating material were used in this study. The thickness that provided the lowest fast-neutrons contribution to the total fluence rate compared to the low-energy component and that allowed delivery of the necessary dose for the reasonable time was investigated.

The proposed carbon reflector consists of two major parts: a side-reflector and a back-reflector. The reflector decreases the neutron leaking and allows getting a higher neutron fluence rate inside a brain phantom. After the scoping calculations using MCNP the 30-cm thick side-reflector and the 22-cm thick back-reflector were chosen for all further analysis.

Neutrons emitted from the ^{18}O target had a certain energy spectrum and angular distribution. These data were used to define the neutron source in MCNP calculations.

The ^{18}O target was also considered as a strong isotropically-emitting gamma-source with known energy spectrum. The dose rates from the neutron and gamma irradiation were determined at different depths inside a brain phantom using MCNP. The phantom was filled with a special composition to simulate brain tissue (ICRU-44 1989) and the tally cells were 0.5 cm diameter spheres at depths of 1, 2, 3, 4, 5, 6, 7 and 8 cm. Most neutrons have been thermalized at the tally depths. So, to know the total dose delivered to the tumor and the healthy tissue, other components of the total dose were calculated. There are two principal capture reactions for thermal neutrons in tissue – $^{1}H(n,\gamma)^{2}H$ and $^{14}N(n,p)^{14}C$ (Turner 1995). These reactions occur both in healthy tissue and tumor and are unwanted irradiation. The main dose component to the tumor, which should be maximized, is the neutron capture reaction with ^{10}B. The charged particles produced in this reaction, $^{10}B(n,\alpha)^{7}Li$, have the total kinetic energy of 2.34 MeV on average and their range in tissue of about 10 μm, the order of the size of a tumor cell. To maximize dose to the tumor and keep the dose to healthy tissue as low as possible, ^{10}B concentrations in normal tissue must be much lower than that within the tumor. B-10 concentrations in healthy tissue of 11.4 ppm and within the tumor of 40 ppm were assumed (Coderre *et al* 1998).

Geometries with several moderating materials having different thicknesses were investigated using MCNP. Two different thicknesses, 25 cm and 30 cm, were investigated for a light water moderator. The results showed that light water heavily absorbed neutrons. Thus, the resulting neutron fluence rates came out to be very low; almost two orders lower than it is desirable for BNCT. Since the neutron fluence rate is

so low, the boron capture provided only a little contribution to the total dose and the therapeutic ratio, which mainly depends on the dose component coming from the neutron capture on boron, was close to 1. Thus, light water cannot be used as a part of the irradiation system for BNCT.

Two thicknesses of carbon moderator were also considered, 30 cm and 40 cm. A 30-cm thick carbon moderator does not provide sufficient moderation of neutrons, so healthy tissue received a significant dose from fast neutrons and as a result the therapeutic ratio was less than 2. A carbon thickness of 40 cm was sufficient to moderate neutrons, but the resulting neutron fluence rates were barely higher than those obtained with a light water moderator. Although the therapeutic ratio was relatively high, this moderating material cannot be used for BNCT, since the treatment time would be 740 minutes, which is extremely high.

Another popular type of a BNCT moderator, called Fluental^{TM}, was investigated. Two different thicknesses of this moderating material were considered. The first calculation was done for a moderator thickness of 30 cm, and the second calculation for 40 cm of Fluental^{TM}. The fluence rates obtained were much higher compared to those of carbon. The use of Fluental^{TM} instead of carbon provided a factor of 1.5 – 2 increase in a total fluence rate but, since the Fluental^{TM} has lower moderation ability, the resulting neutron spectrum suffered from fast neutrons. This results in a huge contribution to the total dose in healthy tissue from fast neutrons. Thus, the therapeutic ratio was less than 2 for a 30-cm thick Fluental^{TM} moderator, which is not enough for successful tumor treatment. The therapeutic ratio for a 40-cm thick moderator was slightly higher than 2,

and the resulting neutron fluence rate provided the treatment time of 277 minutes, which is probably reasonable. Thus, this geometry was considered as one of the possible choices for BNCT.

The most promising results were obtained with a heavy water moderator. Four different thicknesses were investigated – 25, 30, 40 and 50 cm. Neutron fluence rates came out to be higher or at least of the same order of magnitude compared to other types of moderating materials. A 25 cm thickness didn't provide sufficient moderation of neutrons, thus the therapeutic ratio was less than 2. Heavy water moderators with thicknesses of 40 cm and 50 cm could significantly thermalize neutrons, but the resulting fluence rates inside brain were low because of the large source-target distance. The treatment time for a 40-cm thick heavy water moderator would be 537 minutes and for a 50-cm thick – 1050 minutes.

The best results were obtained using a 30-cm thick heavy water moderator. This moderating material provided a relatively high therapeutic ratio for a reasonable treatment time compared to other geometries. Results showed that using of a PETtrace cyclotron in this configuration provides a therapeutic ratio of about 2.4 for depths up to 4 cm inside a brain phantom. A treatment time using a heavy water moderator in this particular geometry would be 258 minutes, assuming a 60 μA beam current. For this treatment time, healthy tissue would get a dose of 12.5 RBEGy and a shallow tumor would get a dose of approximately 30 RBEGy. These results for heavy water appear preferable to a 40-cm thick Fluental^{TM} moderator.

Several calculations were carried out to investigate the advantage of using filtering material such as natural nickel. Two different moderators were selected for a filtering experiment – heavy water and Fluental^{TM}, both having thickness of 30 cm. A 2-cm thick nickel filter was placed at two different depths inside a moderator assembly. As a result, neutron energies were expected to shift to the epithermal region thus reducing the dose to scalp and skull from thermal neutrons and increasing the therapeutic ratio for brain tissue. The filtered fluence rates as well as the therapeutic ratios were lower by 20 – 30 percent compared to those obtained without filtering. Another calculation was made to see a difference between natural nickel filter and a ^{60}Ni filter that has several benefits compared to natural nickel. The use of a ^{60}Ni filter resulted in a higher therapeutic ratio compared to the geometry with a natural nickel filter, but it was still much less than that for the geometry with no filter. Thus, the use of a nickel filter didn't show any benefits in term of therapeutic ratios, and, since the total fluence rate was also reduced, the moderator assembly containing 30-cm thick heavy water and no filter was chosen as most suitable for BNCT using GE PETtrace cyclotron.

Although some positive results in using of this cyclotron were showed in this research, the main disadvantage of GE PETtrace as a neutron source is a low neutron fluence rate. But further increase of a beam current up to 120 μA that proposed by GE should significantly improve the beam quality or improve the treatment time. This lack of neutrons and the condition of a reasonable treatment time have restricted a moderator thickness, thus almost all of the moderating geometries considered suffered from fast neutrons. These neutrons provided significant dose to healthy tissue reducing the

therapeutic ratio. Increasing of a beam current should improve the beam quality by using a moderator of a larger thickness, for example 50 cm. These conditions may be considered in a future work. The therapeutic ratio in this case would be around 3 for the approximately the same treatment time, see Table III-12 above. Also, the photoneutron reaction with heavy water, which can provide additional neutrons to the beam, has not been investigated in this research and thus may be considered for a future work.

The results suggest that it is possible to use this particular cyclotron with this target for the tumor treatment. The data presented in this dissertation allow the conclusion that this type of neutron source should provide acceptable doses and treatment times for tumor irradiation at a depth of up to 4-5 cm inside the brain phantom where the therapeutic ratio is higher than 2.

REFERENCES

Allen D A, Beynon T D 1995 A design study for an accelerator-based epithermal neutron beam for BNCT *Phys. Med. Biol.* **40** 807-821

Allen D A, Beynon T D, Green S 1999 Design for an accelerator-based orthogonal epithermal neutron beam for boron neutron capture therapy *Med. Phys.* **26**(1) 71-76

Allen D A, Beynon T D 2000 What is the best proton energy for accelerator based BNCT using the ^{7}Li(p,n)^{7}Be reaction? *Med. Phys.* **27**(5) 1113-1118

Anderson O A, Kwan J W 1994 Electrostatic quadrupole DC accelerators for BNCT applications *4th Europ. Particle Accelerator Conf.* London LBL-34963, Lawrence Berkeley Laboratory

Auterinen L, Hiismäki P 1993 Epithermal BNCT neutron beam design for a Triga II reactor *The 5th International Symposium on Neutron Capture Therapy* Plenum Press: New York 81-84

Bayanov B F, Belov V P, Bender E D, Bokhovko M V, Dimov G I et al. 1998 Accelerator-based neutron source for the neutron-capture and fast neutron therapy at hospital *Nucl.Instr. and Meth. In Phys. Res.* **A413** 397-426

Bisceglie E, Colangelo P, Colonna N, Santorelli P, Variale V 2000 On the optimal energy of epithermal beams for BNCT *Phys. Med. Biol.* **45** 49-58

Bleuel D L, Donahue R J, Ludewigt B A, Vujic J 1998 Designing accelerator-based epithermal neutron beams for boron neutron capture therapy *Med. Phys.* **25**(9) 1725-1734

Bleuel D L, Chu W T, Donahue R J, Ludewigt B A, McDonald R J et al. 1999 Initial experimental verification of the neutron beam modeling for the LBNL BNCT facility, in application of accelerators in research and industry *Conference Proceedings of the 15th International Conference on Application of Accelerators in Research and Industry (Denton, TX 4 -7 Nov.)* **475** 1050-1055

Briesmeister J F 2000 A general Monte-Carlo n-particle transport code *LA-13709-M* LANL Los Alamos NM

Burlon A A, Kreiner A J, White S M, Blackburn B W, Gierga D P et al. 2001 In-phantom dosimetry for the $^{13}C(d,n)^{14}N$ reaction as a source for accelerator-based BNCT *Med. Phys.* **28**(5) 796-803

Burlon A A, Kreiner A J, Valda A A, Minsky D M 2004 An optimized neutron-beam shaping assembly for accelerator-based BNCT *Applied Radiation and Isotopes* **61** 811-815

Caswell R S, Coyne J J, Randolph M L1980 Kerma factors for neutron energies below 30 MeV *Radiat. Res.* **83** 217-254

Coderre J A, Makar M S, Micca P L, Nawrocky M M, Liu H B et al. 1993 Derivations of relative biological effectiveness for the high-let radiations produced during boron neutron capture irradiations of the 9L rat gliosarcoma in vitro and in vivo *Int. J. Radiat. Oncol. Biol. Phys.* **27** 1121-1129

Coderre J A, Chanana A D, Joel D D, Elowitz E H, Micca P L et al. 1998 Biodistribution of boronophenylalanine in patients with glioblastoma multiforme: boron concentration correlates with tumor cellularity *Radiat. Res.* **149**(2) 163-170

Culbertson C N, Green S, Mason A J, Picton D, Baugh G et al. 2004 In-phantom characterization studies at the Birmingham Accelerator-Generated epIthermal Neutron Source (BAGINS) BNCT facility *Applied Radiation and Isotopes* **61** 733-738

GE Medical Systems 2000 PETtrace Reference Manual *Direction 2131769-100 Rev. 1*

Gritzay O O, Kalchenko O I, Klimova N A, Razbudey V F, Sanzhur A I et al. 2004 Monte-Carlo calculations for the development of a BNCT neutron source at the Kyiv Research Reactor *Appl. Rad. Isot.* **61** 869-873

Harling O K, Roberts K A, Moulin D J, Rogus R D 1995 Head phantoms for neutron capture therapy *Med. Phys.* **22**(5) 579-583

IAEA 2001 Charged-particle cross section database for medical radioisotope production *International Atomic Energy Agency IAEA-TECDOC-1211*

ICRU-44 1989 Tissue substitutes in radiation dosimetry and measurement http://physics.nist.gov/PhysRefData/XrayMassCoef/tab2.html *International Commission on Radiation Units and Measurements*

Kononov O E, Kononov V N, Bokhovko M V, Korobeynikov V V, Soloviev A N et al. 2004 Optimization of an accelerator-based epithermal neutron source for neutron capture therapy *Applied Radiation and Isotopes* **61** 1009-1013

Kudchadker R J, Lee C, Harker Y, Harmon F 1999 Experimental dosimetry and beam evaluation in a phantom for near lithium threshold accelerator-based BNCT *Conference Proceedings of the 15th International Conference on Application of Accelerators in Research and Industry* **475** 1056-1059

Kwan J W, Anderson O A, Reginato L L, Vella M C, Yu S S 1995 A 2.5 MeV electrostatic quadrupole DC accelerator for BNCT application *Nucl. Instr. and Meth. In Phys. Res.* **B99** 710-712

Lundgren K, Ingemannson K 2001 PETtrace-source term evaluations Private Communication (GE Medical Systems)

Mason A, Beynon D, Hopewell J 2001 Beam energies and in phantom dose rates available from the Birmingham BNCT facility *Workshop Proceedings of the 3rd EU-Workshop on Radiobiology of Neutron Capture Therapy (Oxford, UK 17-19 Dec.)* 125-129

Rogus R D, Harling O K, Yanch J C 1994 Mixed field dosimetry of epithermal neutron beams for boron neutron capture therapy at MITR-II research reactor *Med. Phys.* **21** 1611-1625

Tanaka K, Kobayashi T, Sakurai Y, Nakagawa Y, Endo S et al. 2001 Dose distributions in a human head phantom for neutron capture therapy using moderated neutrons from the 2.5 MeV proton-7Li reaction or from fission of 235U *Phys. Med. Biol.* **46**(10) 2681-2695

Tanaka K, Kobayashi T, Sakurai Y, Nakagawa Y, Ishikawa M et al. 2002 Irradiation characteristics of BNCT using near-threshold ^{7}Li(p, n)^{7}Be direct neutrons: application to intra-operative BNCT for malignant brain tumors *Phys. Med. Biol.* **47** 3011-3032

Terlizzi R, Colonna N, Bisceglie E, Colangelo P, Marrone S et al. 2004 Feasibility of an epithermal neutron source for BNCT based on RFQ accelerator *Nucl.Instr. and Meth. In Phys. Res.* **B213** 210-213

Turner J E 1995 *Atoms, Radiation, and Radiation Protection* 2nd Ed. New York: John Wiley and Sons, Inc 370-374

Wang C K, Blue T E, Gahbauer R. 1989 A neutronic study of an accelerator based neutron irradiation facility for boron neutron capture therapy *Nucl. Tech.* **84** 93-107

Yonai S, Aoki T, Nakamura T, Yashima H, Baba M et al. 2003 Feasibility study on epithermal neutron field for cyclotron-based boron neutron capture therapy *Med. Phys.* **30(8)** 2021-2030

Yonai S, Itoga T, Baba M, Nakamura T, Yokobori H et al. 2004 Benchmark experiments for cyclotron-based neutron source for BNCT *Applied Radiation and Isotopes* **61** 997-1001

Zimin S, Allen B J 2000 Study of moderator thickness for an accelerator-based neutron irradiation facility for boron neutron capture therapy using the ^{7}Li(p,n) reaction near threshold *Phys. Med. Biol.* **45** 59-67

APPENDIX A

MCNP INPUT FILE FOR THE NEUTRON DOSE CALCULATION

```
Neutron source with 30 cm D2O moderator thickness
1 8 -1 -1 29 -10 imp:n,p=1 $water (target)
2 12 -7.85 -1 10 -11 imp:n,p=1 $steel cover
3 1 -11.34 -2 11 -12 imp:n,p=1 $lead shield
4 10 -1 13 -3 -16 -14 imp:n,p=1 $moderator
5 3 -2.7 12 -4 -17 -15 #4 imp:n,p=1 $aluminum container
6 5 -2.267 (5 -6 7 -8 12 -15 4):(5 -6 7 -8 -12 11 2):
     (5 -6 7 -8 9 -11 1) imp:n,p=1 $graphite reflector
7 1 -11.34 -4 17 -15 imp:n,p=1 $lead collimator
8 12 -7.85 5 -6 7 -8 18 -9 imp:n,p=1 $steel wall
9 13 -1.04 -20 #10 #14 #15 #16 #17 #18 #19 #20 imp:n,p=1 $phantom
10 13 -1.04 -21 imp:n,p=1 $tumor at 1 cm
14 13 -1.04 -22 imp:n,p=1 $tumor at 2 cm
15 13 -1.04 -23 imp:n,p=1 $tumor at 3 cm
16 13 -1.04 -24 imp:n,p=1 $tumor at 4 cm
17 13 -1.04 -25 imp:n,p=1 $tumor at 5 cm
18 13 -1.04 -26 imp:n,p=1 $tumor at 6 cm
19 13 -1.04 -27 imp:n,p=1 $tumor at 7 cm
20 13 -1.04 -28 imp:n,p=1 $tumor at 8 cm
21 7 -0.001205 (-5:6:-7:8:-18:15) -19 #9 #10 #14 #15 #16
     #17 #18 #19 #20 imp:n,p=1 $air
12 0 19 imp:n,p=0 $vacuum
13 7 -0.001205 -1 9 -29 imp:n,p=1$ target air
```

```
1 cy 5
2 cy 10
3 cy 15
4 cy 16
5 px -46
6 px 46
7 pz -46
8 pz 46
9 py -17
10 py 4
11 py 5
12 py 8
13 py 9
14 py 39
15 py 40
16 ky 60 0.3333333 -1
17 ky 61 0.3333333 -1
18 py -18
19 sy 10 100
20 SQ 0.010412328 0.021626297 0.014515894 0 0 0 -1 0 46 0
21 sy 41.2 0.25
22 sy 42.2 0.25
23 sy 43.2 0.25
24 sy 44.2 0.25
25 sy 45.2 0.25
26 sy 46.2 0.25
27 sy 47.2 0.25
```

```
28 sy 48.2 0.25
29 py 2

mode n p
VOL 8j 2306.889162 11j
AREA 19j 862.075375 9j
c=========================================================================
c                              Source
c=========================================================================
sdef par=1 erg fdir d2 pos=0 2.5 0 dir=d1 vec=0 1 0
si1 L 0.98481 0.86603 0.64279 0.34202 0 -0.34202 -0.64279 -0.86603 -
0.98481
sp1 0.145529955 0.138397972 0.127134436 0.115001384 0.104331861
0.096531728
     0.092077857 0.090519033 0.090475774
ds2 s d3 d4 d5 d6 d7 d8 d9 d10 d11
# si3 sp3
0.000001 0
1 0.048048
2 0.044712
3 0.026989
4 0.013585
5 0.006713
6 0.003139
7 0.001457
8 0.000618
9 0.000269
```

```
# si4 sp4
0.000001 0
1 0.046044
2 0.042598
3 0.025569
4 0.012800
5 0.006291
6 0.002927
7 0.001351
8 0.000569
9 0.000246
# si5 sp5
0.000001 0
1 0.042772
2 0.039255
3 0.023380
4 0.011590
5 0.005642
6 0.002601
7 0.001188
8 0.000495
9 0.000212
# si6 sp6
0.000001 0
1 0.039182
2 0.035638
3 0.021037
```

```
4 0.010308
5 0.004961
6 0.002261
7 0.001019
8 0.000419
9 0.000177
# si7 sp7
0.000001 0
1 0.035964
2 0.032432
3 0.018980
4 0.009206
5 0.004385
6 0.001977
7 0.000880
8 0.000358
9 0.000149
# si8 sp8
0.000001 0
1 0.033545
2 0.030057
3 0.017475
4 0.008429
5 0.003992
6 0.001789
7 0.000792
8 0.000320
```

```
9 0.000133
# si9 sp9
0.000001 0
1 0.032088
2 0.028664
3 0.016612
4 0.008018
5 0.003799
6 0.001704
7 0.000757
8 0.000307
9 0.000128
# si10 sp10
0.000001 0
1 0.031496
2 0.028138
3 0.016309
4 0.007909
5 0.003767
6 0.001698
7 0.000761
8 0.000311
9 0.000131
# si11 sp11
0.000001 0
1 0.031407
2 0.028095
```

```
3 0.016306
4 0.007936
5 0.003793
6 0.001716
7 0.000772
8 0.000317
9 0.000134
c=====================================================================
c                                  Tumor at 1 cm
c=====================================================================
c Photon Fluence in tumor
f4:p 10
fm4 3.21e+11
E4 0.01 0.1 0.2 0.5 1 2 5 10
c Photon RBE-Dose in tumor (rem/hr)
f14:p 10
fm14 3.21e+11
de14 0.01 0.015 0.02 0.03 0.04 0.05 0.06 0.08 0.1 0.15 0.2 0.3 0.4 0.5
     0.6 0.8 1 1.5 2 3 4 5 6 8 10
df14 2.78e-6 1.11e-6 5.88e-7 2.56e-7 1.56e-7 1.2e-7 1.11e-7 1.2e-7
     1.47e-7 2.38e-7 3.45e-7 5.56e-7 7.69e-7 9.09e-7 1.14e-6 1.47e-6
     1.79e-6 2.44e-6 3.03e-6 4e-6 4.76e-6 5.56e-6 6.25e-6 7.69e-6
9.09e-6
c Neutron Fluence in tumor
f24:n 10
fm24 3.21e+11
E24 0.0000005 0.000001 0.00001 0.0001 .001 .01 .1 1 10
```

```
c RBE-Dose in tumor (rem/hr)
f34:n 10
fm34 3.21e+11
de34 2.5e-8 1e-7 1e-6 1e-5 1e-4 1e-3 1e-2 1e-1 5e-1 1 2.5 5 7 10
df34 3.67e-6 3.67e-6 4.46e-6 4.54e-6 4.18e-6 3.76e-6 3.56e-6 2.17e-5
     9.26e-5 1.32e-4 1.25e-4 1.56e-4 1.47e-4 1.47e-4
c=========================================================================
c                                  Tumor at 2 cm
c=========================================================================
c Photon Fluence in tumor
f44:p 14
fm44 3.21e+11
E44 0.01 0.1 0.2 0.5 1 2 5 10
c Photon RBE-Dose in tumor (rem/hr)
f54:p 14
fm54 3.21e+11
de54 0.01 0.015 0.02 0.03 0.04 0.05 0.06 0.08 0.1 0.15 0.2 0.3 0.4 0.5
     0.6 0.8 1 1.5 2 3 4 5 6 8 10
df54 2.78e-6 1.11e-6 5.88e-7 2.56e-7 1.56e-7 1.2e-7 1.11e-7 1.2e-7
     1.47e-7 2.38e-7 3.45e-7 5.56e-7 7.69e-7 9.09e-7 1.14e-6 1.47e-6
     1.79e-6 2.44e-6 3.03e-6 4e-6 4.76e-6 5.56e-6 6.25e-6 7.69e-6
9.09e-6
c Neutron Fluence in tumor
f64:n 14
fm64 3.21e+11
E64 0.0000005 0.000001 0.00001 0.0001 .001 .01 .1 1 10
c RBE-Dose in tumor (rem/hr)
```

```
f74:n 14
fm74 3.21e+11
de74 2.5e-8 1e-7 1e-6 1e-5 1e-4 1e-3 1e-2 1e-1 5e-1 1 2.5 5 7 10
df74 3.67e-6 3.67e-6 4.46e-6 4.54e-6 4.18e-6 3.76e-6 3.56e-6 2.17e-5
     9.26e-5 1.32e-4 1.25e-4 1.56e-4 1.47e-4 1.47e-4
c======================================================================
c                                  Tumor at 3 cm
c======================================================================
c Photon Fluence in tumor
f84:p 15
fm84 3.21e+11
E84 0.01 0.1 0.2 0.5 1 2 5 10
c Photon RBE-Dose in tumor (rem/hr)
f94:p 15
fm94 3.21e+11
de94 0.01 0.015 0.02 0.03 0.04 0.05 0.06 0.08 0.1 0.15 0.2 0.3 0.4 0.5
     0.6 0.8 1 1.5 2 3 4 5 6 8 10
df94 2.78e-6 1.11e-6 5.88e-7 2.56e-7 1.56e-7 1.2e-7 1.11e-7 1.2e-7
     1.47e-7 2.38e-7 3.45e-7 5.56e-7 7.69e-7 9.09e-7 1.14e-6 1.47e-6
     1.79e-6 2.44e-6 3.03e-6 4e-6 4.76e-6 5.56e-6 6.25e-6 7.69e-6
9.09e-6
c Neutron Fluence in tumor
f104:n 15
fm104 3.21e+11
E104 0.0000005 0.000001 0.00001 0.0001 .001 .01 .1 1 10
c RBE-Dose in tumor (rem/hr)
f114:n 15
```

```
fm114 3.21e+11
de114 2.5e-8 1e-7 1e-6 1e-5 1e-4 1e-3 1e-2 1e-1 5e-1 1 2.5 5 7 10
df114 3.67e-6 3.67e-6 4.46e-6 4.54e-6 4.18e-6 3.76e-6 3.56e-6 2.17e-5
     9.26e-5 1.32e-4 1.25e-4 1.56e-4 1.47e-4 1.47e-4
c======================================================================
c                                  Tumor at 4 cm
c======================================================================
c Photon Fluence in tumor
f124:p 16
fm124 3.21e+11
E124 0.01 0.1 0.2 0.5 1 2 5 10
c Photon RBE-Dose in tumor (rem/hr)
f134:p 16
fm134 3.21e+11
de134 0.01 0.015 0.02 0.03 0.04 0.05 0.06 0.08 0.1 0.15 0.2 0.3 0.4 0.5
     0.6 0.8 1 1.5 2 3 4 5 6 8 10
df134 2.78e-6 1.11e-6 5.88e-7 2.56e-7 1.56e-7 1.2e-7 1.11e-7 1.2e-7
     1.47e-7 2.38e-7 3.45e-7 5.56e-7 7.69e-7 9.09e-7 1.14e-6 1.47e-6
     1.79e-6 2.44e-6 3.03e-6 4e-6 4.76e-6 5.56e-6 6.25e-6 7.69e-6
9.09e-6
c Neutron Fluence in tumor
f144:n 16
fm144 3.21e+11
E144 0.0000005 0.000001 0.00001 0.0001 .001 .01 .1 1 10
c RBE-Dose in tumor (rem/hr)
f154:n 16
fm154 3.21e+11
```

```
de154 2.5e-8 1e-7 1e-6 1e-5 1e-4 1e-3 1e-2 1e-1 5e-1 1 2.5 5 7 10
df154 3.67e-6 3.67e-6 4.46e-6 4.54e-6 4.18e-6 3.76e-6 3.56e-6 2.17e-5
     9.26e-5 1.32e-4 1.25e-4 1.56e-4 1.47e-4 1.47e-4
c=======================================================================
c                                  Tumor at 5 cm
c=======================================================================
c Photon Fluence in tumor
f164:p 17
fm164 3.21e+11
E164 0.01 0.1 0.2 0.5 1 2 5 10
c Photon RBE-Dose in tumor (rem/hr)
f174:p 17
fm174 3.21e+11
de174 0.01 0.015 0.02 0.03 0.04 0.05 0.06 0.08 0.1 0.15 0.2 0.3 0.4 0.5
     0.6 0.8 1 1.5 2 3 4 5 6 8 10
df174 2.78e-6 1.11e-6 5.88e-7 2.56e-7 1.56e-7 1.2e-7 1.11e-7 1.2e-7
     1.47e-7 2.38e-7 3.45e-7 5.56e-7 7.69e-7 9.09e-7 1.14e-6 1.47e-6
     1.79e-6 2.44e-6 3.03e-6 4e-6 4.76e-6 5.56e-6 6.25e-6 7.69e-6
9.09e-6
c Neutron Fluence in tumor
f184:n 17
fm184 3.21e+11
E184 0.0000005 0.000001 0.00001 0.0001 .001 .01 .1 1 10
c RBE-Dose in tumor (rem/hr)
f194:n 17
fm194 3.21e+11
de194 2.5e-8 1e-7 1e-6 1e-5 1e-4 1e-3 1e-2 1e-1 5e-1 1 2.5 5 7 10
```

```
df194 3.67e-6 3.67e-6 4.46e-6 4.54e-6 4.18e-6 3.76e-6 3.56e-6 2.17e-5
     9.26e-5 1.32e-4 1.25e-4 1.56e-4 1.47e-4 1.47e-4
c=====================================================================
c                                  Tumor at 6 cm
c=====================================================================
c Photon Fluence in tumor
f204:p 18
fm204 3.21e+11
E204 0.01 0.1 0.2 0.5 1 2 5 10
c Photon RBE-Dose in tumor (rem/hr)
f214:p 18
fm214 3.21e+11
de214 0.01 0.015 0.02 0.03 0.04 0.05 0.06 0.08 0.1 0.15 0.2 0.3 0.4 0.5
     0.6 0.8 1 1.5 2 3 4 5 6 8 10
df214 2.78e-6 1.11e-6 5.88e-7 2.56e-7 1.56e-7 1.2e-7 1.11e-7 1.2e-7
     1.47e-7 2.38e-7 3.45e-7 5.56e-7 7.69e-7 9.09e-7 1.14e-6 1.47e-6
     1.79e-6 2.44e-6 3.03e-6 4e-6 4.76e-6 5.56e-6 6.25e-6 7.69e-6
9.09e-6
c Neutron Fluence in tumor
f224:n 18
fm224 3.21e+11
E224 0.0000005 0.000001 0.00001 0.0001 .001 .01 .1 1 10
c RBE-Dose in tumor (rem/hr)
f234:n 18
fm234 3.21e+11
de234 2.5e-8 1e-7 1e-6 1e-5 1e-4 1e-3 1e-2 1e-1 5e-1 1 2.5 5 7 10
df234 3.67e-6 3.67e-6 4.46e-6 4.54e-6 4.18e-6 3.76e-6 3.56e-6 2.17e-5
```

```
     9.26e-5 1.32e-4 1.25e-4 1.56e-4 1.47e-4 1.47e-4
c=========================================================================
c                                  Tumor at 7 cm
c=========================================================================
c Photon Fluence in tumor
f244:p 19
fm244 3.21e+11
E244 0.01 0.1 0.2 0.5 1 2 5 10
c Photon RBE-Dose in tumor (rem/hr)
f254:p 19
fm254 3.21e+11
de254 0.01 0.015 0.02 0.03 0.04 0.05 0.06 0.08 0.1 0.15 0.2 0.3 0.4 0.5
     0.6 0.8 1 1.5 2 3 4 5 6 8 10
df254 2.78e-6 1.11e-6 5.88e-7 2.56e-7 1.56e-7 1.2e-7 1.11e-7 1.2e-7
     1.47e-7 2.38e-7 3.45e-7 5.56e-7 7.69e-7 9.09e-7 1.14e-6 1.47e-6
     1.79e-6 2.44e-6 3.03e-6 4e-6 4.76e-6 5.56e-6 6.25e-6 7.69e-6
9.09e-6
c Neutron Fluence in tumor
f264:n 19
fm264 3.21e+11
E264 0.0000005 0.000001 0.00001 0.0001 .001 .01 .1 1 10
c RBE-Dose in tumor (rem/hr)
f274:n 19
fm274 3.21e+11
de274 2.5e-8 1e-7 1e-6 1e-5 1e-4 1e-3 1e-2 1e-1 5e-1 1 2.5 5 7 10
df274 3.67e-6 3.67e-6 4.46e-6 4.54e-6 4.18e-6 3.76e-6 3.56e-6 2.17e-5
     9.26e-5 1.32e-4 1.25e-4 1.56e-4 1.47e-4 1.47e-4
```

```
c=====================================================================
c                                  Tumor at 8 cm
c=====================================================================
c Photon Fluence in tumor
f284:p 20
fm284 3.21e+11
E284 0.01 0.1 0.2 0.5 1 2 5 10
c Photon RBE-Dose in tumor (rem/hr)
f294:p 20
fm294 3.21e+11
de294 0.01 0.015 0.02 0.03 0.04 0.05 0.06 0.08 0.1 0.15 0.2 0.3 0.4 0.5
     0.6 0.8 1 1.5 2 3 4 5 6 8 10
df294 2.78e-6 1.11e-6 5.88e-7 2.56e-7 1.56e-7 1.2e-7 1.11e-7 1.2e-7
     1.47e-7 2.38e-7 3.45e-7 5.56e-7 7.69e-7 9.09e-7 1.14e-6 1.47e-6
     1.79e-6 2.44e-6 3.03e-6 4e-6 4.76e-6 5.56e-6 6.25e-6 7.69e-6
9.09e-6
c Neutron Fluence in tumor
f304:n 20
fm304 3.21e+11
E304 0.0000005 0.000001 0.00001 0.0001 .001 .01 .1 1 10
c RBE-Dose in tumor (rem/hr)
f314:n 20
fm314 3.21e+11
de314 2.5e-8 1e-7 1e-6 1e-5 1e-4 1e-3 1e-2 1e-1 5e-1 1 2.5 5 7 10
df314 3.67e-6 3.67e-6 4.46e-6 4.54e-6 4.18e-6 3.76e-6 3.56e-6 2.17e-5
     9.26e-5 1.32e-4 1.25e-4 1.56e-4 1.47e-4 1.47e-4
c=====================================================================
```

```
c                                   Material Cards
c=======================================================================
M1 82207 1 $lead
M3 13027.21c 1 $aluminum
M5 6012.21c 1 $carbon
M7 6012.21c -0.000124 7014.60c -0.755268 8016.60c -0.231781 18000.42c -
0.012827 $air
M8 1001.60c -0.111898 8016.60c -0.888102 $target
c M9 13027 -0.432 9019 -0.559 3007 -0.009 $aluminum/fluorine/lithium
moderator
M10 1002.60c -0.2 8016.60c -0.8 $d2o
c M11 4009.60c 1 8016.60c 1 $BeO
M12 24000.42c -0.12 26000.21c -0.8775 6012.21c -0.0025 $steel
M13 1001.60c -0.107 6012.21c -0.145 7014.60c -0.022 8016.60c -0.712
     11023.60c -0.002 15031.60c -0.004 16000.60c -0.002 17000.60c -
0.003
     19000.60c -0.003 $brain
CTME 10000
```

APPENDIX B

MCNP INPUT FILE FOR THE PHOTON DOSE CALCULATION

```
Isotropic source with 30 cm moderator (Fluental) thickness
1 8 -1 -1 29 -10 imp:n,p=1 $water (target)
2 12 -7.85 -1 10 -11 imp:n,p=1 $steel cover
3 1 -11.34 -2 11 -12 imp:n,p=1 $lead shield
4 10 -1 13 -3 -16 -14 imp:n,p=1 $moderator heavy water
5 3 -2.7 12 -4 -17 -15 #4 imp:n,p=1 $aluminum container
6 5 -2.267 (5 -6 7 -8 12 -15 4):(5 -6 7 -8 -12 11 2):
      (5 -6 7 -8 9 -11 1) imp:n,p=1 $graphite reflector
7 1 -11.34 -4 17 -15 imp:n,p=1 $lead collimator
8 12 -7.85 5 -6 7 -8 18 -9 imp:n,p=1 $steel wall
9 13 -1.04 -20 #10 #14 #15 #16 #17 #18 #19 #20 imp:n,p=1 $phantom
10 13 -1.04 -21 imp:n,p=1 $tumor at 1 cm
14 13 -1.04 -22 imp:n,p=1 $tumor at 2 cm
15 13 -1.04 -23 imp:n,p=1 $tumor at 3 cm
16 13 -1.04 -24 imp:n,p=1 $tumor at 4 cm
17 13 -1.04 -25 imp:n,p=1 $tumor at 5 cm
18 13 -1.04 -26 imp:n,p=1 $tumor at 6 cm
19 13 -1.04 -27 imp:n,p=1 $tumor at 7 cm
20 13 -1.04 -28 imp:n,p=1 $tumor at 8 cm
21 7 -0.001205 (-5:6:-7:8:-18:15) -19 #9 #10 #14 #15 #16
      #17 #18 #19 #20 imp:n,p=1 $air
12 0 19 imp:n,p=0 $vacuum
13 7 -0.001205 -1 9 -29 imp:n,p=1$ target air
1 cy 5
```

```
2 cy 10

3 cy 15

4 cy 16

5 px -46

6 px 46

7 pz -46

8 pz 46

9 py -17

10 py 3

11 py 4

12 py 8

13 py 9

14 py 39

15 py 40

16 ky 60 0.3333333 -1

17 ky 61 0.3333333 -1

18 py -18

19 sy 10 100

20 SQ 0.010412328 0.021626297 0.014515894 0 0 0 -1 0 47 0

21 sy 41.2 0.25

22 sy 42.2 0.25

23 sy 43.2 0.25

24 sy 44.2 0.25

25 sy 45.2 0.25

26 sy 46.2 0.25

27 sy 47.2 0.25

28 sy 48.2 0.25
```

```
29 py 2


mode p
VOL 8j 2306.889162 11j
AREA 19j 862.075375 9j
c=========================================================================
c                              Isotropic Photon Source
c=========================================================================
sdef par=2 erg=d1 pos=0 2.5 0
# si1 sp1
0.001 0
1 8.8e+11
2 7.4e+11
3 2.6e+11
4 1.6e+11
5 8.7e+10
6 4.6e+10
7 2.2e+10
8 8.8e+9
9 2e+9
c=========================================================================
c                                  Tumor at 1 cm
c=========================================================================
c Photon Fluence in tumor
f4:p 10
fm4 2.206e+12
E4 0.01 0.1 0.2 0.5 1 2 5 10
```

```
c Photon RBE-Dose in tumor (rem/hr)
f14:p 10
fm14 2.206e+12
de14 0.01 0.015 0.02 0.03 0.04 0.05 0.06 0.08 0.1 0.15 0.2 0.3 0.4 0.5
     0.6 0.8 1 1.5 2 3 4 5 6 8 10
df14 2.78e-6 1.11e-6 5.88e-7 2.56e-7 1.56e-7 1.2e-7 1.11e-7 1.2e-7
     1.47e-7 2.38e-7 3.45e-7 5.56e-7 7.69e-7 9.09e-7 1.14e-6 1.47e-6
     1.79e-6 2.44e-6 3.03e-6 4e-6 4.76e-6 5.56e-6 6.25e-6 7.69e-6
9.09e-6
c======================================================================
c                                  Tumor at 2 cm
c======================================================================
c Photon Fluence in tumor
f44:p 14
fm44 2.206e+12
E44 0.01 0.1 0.2 0.5 1 2 5 10
c Photon RBE-Dose in tumor (rem/hr)
f54:p 14
fm54 2.206e+12
de54 0.01 0.015 0.02 0.03 0.04 0.05 0.06 0.08 0.1 0.15 0.2 0.3 0.4 0.5
     0.6 0.8 1 1.5 2 3 4 5 6 8 10
df54 2.78e-6 1.11e-6 5.88e-7 2.56e-7 1.56e-7 1.2e-7 1.11e-7 1.2e-7
     1.47e-7 2.38e-7 3.45e-7 5.56e-7 7.69e-7 9.09e-7 1.14e-6 1.47e-6
     1.79e-6 2.44e-6 3.03e-6 4e-6 4.76e-6 5.56e-6 6.25e-6 7.69e-6
9.09e-6
c======================================================================
c                                  Tumor at 3 cm
```

```
c=====================================================================
c Photon Fluence in tumor
f84:p 15
fm84 2.206e+12
E84 0.01 0.1 0.2 0.5 1 2 5 10
c Photon RBE-Dose in tumor (rem/hr)
f94:p 15
fm94 2.206e+12
de94 0.01 0.015 0.02 0.03 0.04 0.05 0.06 0.08 0.1 0.15 0.2 0.3 0.4 0.5
     0.6 0.8 1 1.5 2 3 4 5 6 8 10
df94 2.78e-6 1.11e-6 5.88e-7 2.56e-7 1.56e-7 1.2e-7 1.11e-7 1.2e-7
     1.47e-7 2.38e-7 3.45e-7 5.56e-7 7.69e-7 9.09e-7 1.14e-6 1.47e-6
     1.79e-6 2.44e-6 3.03e-6 4e-6 4.76e-6 5.56e-6 6.25e-6 7.69e-6
9.09e-6
c=====================================================================
c                                  Tumor at 4 cm
c=====================================================================
c Photon Fluence in tumor
f124:p 16
fm124 2.206e+12
E124 0.01 0.1 0.2 0.5 1 2 5 10
c Photon RBE-Dose in tumor (rem/hr)
f134:p 16
fm134 2.206e+12
de134 0.01 0.015 0.02 0.03 0.04 0.05 0.06 0.08 0.1 0.15 0.2 0.3 0.4 0.5
     0.6 0.8 1 1.5 2 3 4 5 6 8 10
df134 2.78e-6 1.11e-6 5.88e-7 2.56e-7 1.56e-7 1.2e-7 1.11e-7 1.2e-7
```

```
     1.47e-7 2.38e-7 3.45e-7 5.56e-7 7.69e-7 9.09e-7 1.14e-6 1.47e-6
     1.79e-6 2.44e-6 3.03e-6 4e-6 4.76e-6 5.56e-6 6.25e-6 7.69e-6
9.09e-6
c=====================================================================
c                                  Tumor at 5 cm
c=====================================================================
c Photon Fluence in tumor
f164:p 17
fm164 2.206e+12
E164 0.01 0.1 0.2 0.5 1 2 5 10
c Photon RBE-Dose in tumor (rem/hr)
f174:p 17
fm174 2.206e+12
de174 0.01 0.015 0.02 0.03 0.04 0.05 0.06 0.08 0.1 0.15 0.2 0.3 0.4 0.5
     0.6 0.8 1 1.5 2 3 4 5 6 8 10
df174 2.78e-6 1.11e-6 5.88e-7 2.56e-7 1.56e-7 1.2e-7 1.11e-7 1.2e-7
     1.47e-7 2.38e-7 3.45e-7 5.56e-7 7.69e-7 9.09e-7 1.14e-6 1.47e-6
     1.79e-6 2.44e-6 3.03e-6 4e-6 4.76e-6 5.56e-6 6.25e-6 7.69e-6
9.09e-6
c=====================================================================
c                                  Tumor at 6 cm
c=====================================================================
c Photon Fluence in tumor
f204:p 18
fm204 2.206e+12
E204 0.01 0.1 0.2 0.5 1 2 5 10
c Photon RBE-Dose in tumor (rem/hr)
```

```
f214:p 18
fm214 2.206e+12
de214 0.01 0.015 0.02 0.03 0.04 0.05 0.06 0.08 0.1 0.15 0.2 0.3 0.4 0.5
     0.6 0.8 1 1.5 2 3 4 5 6 8 10
df214 2.78e-6 1.11e-6 5.88e-7 2.56e-7 1.56e-7 1.2e-7 1.11e-7 1.2e-7
     1.47e-7 2.38e-7 3.45e-7 5.56e-7 7.69e-7 9.09e-7 1.14e-6 1.47e-6
     1.79e-6 2.44e-6 3.03e-6 4e-6 4.76e-6 5.56e-6 6.25e-6 7.69e-6
9.09e-6
c=====================================================================
c                                  Tumor at 7 cm
c=====================================================================
c Photon Fluence in tumor
f244:p 19
fm244 2.206e+12
E244 0.01 0.1 0.2 0.5 1 2 5 10
c Photon RBE-Dose in tumor (rem/hr)
f254:p 19
fm254 2.206e+12
de254 0.01 0.015 0.02 0.03 0.04 0.05 0.06 0.08 0.1 0.15 0.2 0.3 0.4 0.5
     0.6 0.8 1 1.5 2 3 4 5 6 8 10
df254 2.78e-6 1.11e-6 5.88e-7 2.56e-7 1.56e-7 1.2e-7 1.11e-7 1.2e-7
     1.47e-7 2.38e-7 3.45e-7 5.56e-7 7.69e-7 9.09e-7 1.14e-6 1.47e-6
     1.79e-6 2.44e-6 3.03e-6 4e-6 4.76e-6 5.56e-6 6.25e-6 7.69e-6
9.09e-6
c=====================================================================
c                                  Tumor at 8 cm
c=====================================================================
```

```
c Photon Fluence in tumor
f284:p 20
fm284 2.206e+12
E284 0.01 0.1 0.2 0.5 1 2 5 10
c Photon RBE-Dose in tumor (rem/hr)
f294:p 20
fm294 2.206e+12
de294 0.01 0.015 0.02 0.03 0.04 0.05 0.06 0.08 0.1 0.15 0.2 0.3 0.4 0.5
     0.6 0.8 1 1.5 2 3 4 5 6 8 10
df294 2.78e-6 1.11e-6 5.88e-7 2.56e-7 1.56e-7 1.2e-7 1.11e-7 1.2e-7
     1.47e-7 2.38e-7 3.45e-7 5.56e-7 7.69e-7 9.09e-7 1.14e-6 1.47e-6
     1.79e-6 2.44e-6 3.03e-6 4e-6 4.76e-6 5.56e-6 6.25e-6 7.69e-6
9.09e-6
c=====================================================================
c                                  Material Cards
c=====================================================================
M1 82000 1 $lead
M3 13000 1 $aluminum
M5 6000 1 $carbon
M7 6000 -0.000124 7000 -0.755268 8000 -0.231781 18000 -0.012827 $air
M8 1000 -0.111898 8000 -0.888102 $target
c M9 13027 -0.432 9019 -0.559 3007 -0.009 $aluminum/fluorine/lithium
moderator
M10 1000 -0.2 8000 -0.8 $d2o
c M11 4000 1 8000 1 $BeO
M12 24000 -0.12 26000 -0.8775 6012 -0.0025 $steel
M13 1000 -0.107 6000 -0.145 7000 -0.022 8000 -0.712
```

```
      11000 -0.002 15000 -0.004 16000 -0.002 17000 -0.003
      19000 -0.003 $brain
CTME 10000
```

VITA

Andrey Bosko was born in Pabrade, Lithuania on June 20, 1977. He attended several schools in Russia graduating from Gusinoe Ozero High, Russia in May of 1994. He attended the Moscow Engineering Physics Institute (technical university), Moscow, Russia from September 1977 to June 2000 receiving a Bachelor's of Science in nuclear engineering in June 1998 and a Master's of Science in Nuclear Engineering (nuclear materials safe management) in June 2000. Andrey was admitted to graduate school at Texas A&M University in September 2001 and successfully passed the qualifying exam to enter the Ph.D. program in September 2003. He was employed by the Nuclear Science Center as a Graduate Research Assistant in January 2002.

He received a Doctor of Philosophy degree in nuclear engineering from Texas A&M University in August 2005.

His area of interest in the field of nuclear engineering includes dose evaluation, radiation detection, and reactor experiments.

In the future Mr. Bosko may be reached by writing to the Nuclear Science Center, 1095 Nuclear Science Rd., 3575 TAMU, College Station, TX, 77843-3575.